# REPORT DOCUMENTATION PAGE

*Form Approved*
*OMB No. 0704-0188*



| **1. REPORT DATE** *(DD-MM-YYYY)* | **2. REPORT TYPE** | **3. DATES COVERED** *(From - To)* |
|---|---|---|
| 04-03-2011 | Journal Article | |

**4. TITLE AND SUBTITLE**

**Chemical Kinetics Interpretation of Hypergolicity of Dicyanamide Ionic Liquid-based Systems (Pre-print)**

**5a. CONTRACT NUMBER**
FA8655-07-M-4009

**5b. GRANT NUMBER**

**5c. PROGRAM ELEMENT NUMBER**

**6. AUTHOR(S)**
Laurent Catoire (ICARE, INSRS-CNRS, Univ. of Orleans, ENSTA ParisTech),
Steven D. Chambreau (ERC), and Ghanshyam L. Vaghjiani (AFRL/RZSP)

**5d. PROJECT NUMBER**

**5f. WORK UNIT NUMBER**
**23030423**

**7. PERFORMING ORGANIZATION NAME(S) AND ADDRESS(ES)**

ICARE, INSIS-CNRS, Univ. of Orleans
1C, avenue de la Recherche Scientifique,
45071 Orleans, France

ERC Incorporated
10 E. Saturn Blvd.
Edwards AFB, CA 93524, USA

**8. PERFORMING ORGANIZATION REPORT NUMBER**

AFRL-RZ-ED-JA-2011-067

**9. SPONSORING / MONITORING AGENCY NAME(S) AND ADDRESS(ES)**

Air Force Research Laboratory (AFMC)
AFRL/RZS
5 Pollux Drive
Edwards AFB CA 93524-7048

**10. SPONSOR/MONITOR'S ACRONYM(S)**

**11. SPONSOR/MONITOR'S NUMBER(S)**
AFRL-RZ-ED-JA-2011-067

**12. DISTRIBUTION / AVAILABILITY STATEMENT**

Distribution A: Approved for public release; distribution unlimited (PA #10879).

**13. SUPPLEMENTARY NOTES**
For publication in Combustion and Flame, August 2011

**14. ABSTRACT**

A detailed chemical kinetics model has been built to examine the gas-phase chemistry between isocyanic acid (HNCO), white fuming nitric acid (WFNA), $N_2O$, $CO_2$ and water. This kinetics model is able to explain the gas-phase ignition observed during hypergolic ignition of the ionic liquid; 1-butyl-3-methyl-imidazolium dicyanamide with WFNA. Sensitivity analyses have been performed to examine the reaction pathways for ignition. Ignition is predicted to occur via an exothermic reaction between isocyanic acid (HNCO) and nitric acid ($HONO_2$), and subsequent $HONO_2$ thermal decomposition that has $NO_2$ and OH radicals as the primary chain carriers. A detailed understanding of the initiation processes in the liquid phase is needed as the 1-butyl-3-methyl-imidazolium dicyanamide and WFNA begin to react to produce the above pre-ignition species for the proposed chemical kinetics model to describe the ignition behavior of the system.

**15. SUBJECT TERMS**

| **16. SECURITY CLASSIFICATION OF:** | | | **17. LIMITATION OF ABSTRACT** | **18. NUMBER OF PAGES** | **19a. NAME OF RESPONSIBLE PERSON** |
|---|---|---|---|---|---|
| | | | | | Dr. Ganshyam Vaghjiani |
| **a. REPORT** | **b. ABSTRACT** | **c. THIS PAGE** | | | **19b. TELEPHONE NUMBER** *(include area code)* |
| **Unclassified** | **Unclassified** | **Unclassified** | SAR | 59 | N/A |

# Chemical Kinetics Interpretation of Hypergolicity of Dicyanamide Ionic Liquid-based Systems

Laurent Catoire,[a,b] Steven D. Chambreau,[c] and Ghanshyam L. Vaghjiani[d]

[a]ICARE, INSIS-CNRS, and University of Orleans, 1C, avenue de la Recherche Scientifique, 45071 Orleans, France

[b]ENSTA ParisTech, 32, boulevard Victor, 75739 Paris Cedex 15, France

[c]ERC Incorporated, 10 E. Saturn Blvd., Edwards AFB, CA 93524, USA

[d]Air Force Research Laboratory, Propellants Branch (AFRL/RZSP), 10 E. Saturn Blvd., Edwards AFB, CA 92524, USA

## Abstract

A detailed chemical kinetics model has been built to examine the gas-phase chemistry between isocyanic acid (HNCO), white fuming nitric acid (WFNA), $N_2O$, $CO_2$ and water. This kinetics model is able to explain the gas-phase ignition observed during hypergolic ignition of the ionic liquid; 1-butyl-3-methyl-imidazolium dicyanamide with WFNA. Sensitivity analyses have been performed to examine the reaction pathways for ignition. Ignition is predicted to occur via an exothermic reaction between isocyanic acid (HNCO) and nitric acid ($HONO_2$), and subsequent $HONO_2$ thermal decomposition that has $NO_2$ and OH radicals as the primary chain carriers. A detailed understanding of the initiation processes in the liquid phase is needed as the 1-butyl-3-methyl-imidazolium dicyanamide and WFNA begin to react to produce the above pre-ignition species for the proposed chemical kinetics model to describe the ignition behavior of the system.

*Keywords*: Ionic liquids, ILs, Combustion, Ignition, Hypergolicity

## 1. Introduction

Meeting energy demands while minimizing environmental impact is a major challenge for the 21st century. Pollution and greenhouse effects mostly due to the combustion of fossil fuels and disappearance of easily accessible fossil fuel reservoirs and other combustible materials have led to the search for new fuels that promise to be environmentally benign as well as have superior energy content. Some of these new fuel materials may not be totally "green" but they address, at least partially, some of the drawbacks of the current fuels and combustibles. This ecological emphasis is not limited to auto fuels but extends to all fuels and combustibles, including space propulsion fuels. One of the most utilized bipropellant combinations in the propulsion of satellites and interplanetary vehicles, mono methylhydrazine (MMH)/nitrogen tetroxide (NTO) falls under this scope. These propellants are earth-storable liquids (non-cryogenic), but their vapors are carcinogenic and toxic. MMH's positive enthalpy of formation enables it to sustain a decomposition flame, and therefore can be considered to be more hazardous than conventional fuels which have negative enthalpies of formation. Furthermore, MMH compatibility is often very poor with many materials, and upon its contact with these, it can rapidly decompose exothermically. Similarly, NTO is also known to be corrosive to many materials. It would appear from the above facts that there are numerous valid practical reasons to replace MMH by other fuels that, at least, reduce the risks in handling, storing and transporting the fuel. Finding NTO replacements is also of interest and under certain circumstances the use of nitric acid or other suitable oxidants may be advantageous. Among some of the alternatives proposed to replace MMH are ionic liquids (ILs). ILs exhibit low vapor pressures, an advantage compared to MMH because this ensures limited explosion risks and personnel exposure to potentially toxic and carcinogenic vapors.

The most interesting feature of MMH in combination with NTO is that it is hypergolic, that is, MMH and NTO form mixtures that auto-ignite at room temperature and at low pressures. This characteristic is known to provide high reliability in engine startups for numerous satellite propulsion systems since no external devices (such as ignition sparks) are required to ignite the MMH/NTO combination. Over the last 15 years, the theoretical understanding of hypergolicity in MMH/NTO has sufficiently matured to allow for reasonable predictions in the ignition delay time, a quantity of significant importance in the design of hypergolic engines.**[1-5]** The prospect of similarly predicting ignition delay times for recently discovered and new **[6,7]** ionic liquid hypergols will require a detailed understanding of the underlying chemical pathways and the reaction mechanisms involved when ILs are treated with NTO or any other suitable oxidizer such as red fuming nitric acid (RFNA), white fuming nitric acid (WFNA) or even hydrogen peroxide. Comprehensive gas-phase thermodynamics and chemical kinetics databases will need to be developed since the literature is sparse in this area.

*1.1. General description of ILs*

ILs are synthesized by the reaction of a base with a strong acid. ILs are therefore salts and consist of cations and anions. Each ion and counter ion in the IL will have its own unique chemical and physical attributes, and in a combination, the choice of cation-anion pairs can lead to approximately $10^{18}$ different ionic liquids having, in principle, any desirable or tunable property**.** The number of ILs reported in the literature has expanded almost exponentially over the past two decades, as have their applications ranging from use in electro-deposition of metals, fuel desulphurization, propellants, fuel cells, etc.**[8]** Theoretical tools have been recently developed to understand some of the ILs' physical and thermodynamical properties

to better target the utility of known ILs for the given industrial process under consideration**.** Similarly, new simulation tools will need to be developed to predict those physicochemical properties that allow for an efficient approach to the screening and designing of ILs for hypergolic applications.

*1.2. Requirements for energetic ILs*

In propulsion applications, ILs could have several advantages compared to the existing hypergolic fuel, hydrazine ($N_2H_4$) and its methylated derivatives MMH and UDMH (unsymmetrical dimethylhydrazine, $(CH_3)_2NNH_2$)). ILs have been regarded to be thermally stable, and shown to have negligibly low vapor pressures,**[9]** high densities and large liquid ranges.**[10]** For energetic ILs, the triazolium and tetrazolium cations and their corresponding substituted analogues have been preferred. The anionic counterparts are generally the nitrate ($NO_3^-$), the perchlorate ($ClO_4^-$) or the dinitramide ($N(NO_2)_2^-$) ions. For hypergolic applications, additional anions that exhibit high reactivity with oxidizers need to be considered.**[7]** An exhaustive bibliographic search shows that physiochemical property data exists only for a relatively few compounds, even for such basic properties such as densities and melting points. The preferred performance requirements for energetic ILs in terms of melting point, surface tension, density, viscosity, etc. have recently been reported by Smiglak et al.**[10]**

*1.3. Ignition and combustion of ILs*

Jones et al.**[11]** have reported self-sustained burning of 1-ethyl-4,5-dimethyltetrazolium tetranitratoaluminate by thermal heating of the ionic liquid to about 200°C. An ignition delay

of a few seconds was observed. As a monopropellant, this IL is reported to have a better performance measure than hydrazine.**[11]** Li and Litzinger **[12]** have observed laser-driven self-ignition of 1H-4-amino-1,2,4-triazolium nitrate vapors in air at atmospheric pressure. Ignition occurred when the heat flux reached ~150 W $cm^{-2}$, and in helium, ignition occurred at a flux of ~200 W $cm^{-2}$. Images of the reported ignition in air show that the solid ionic liquid first melts with bubbling, then vaporizes ("smoke" observed) and finally ignites in the gas phase. Alfano et al.**[13]** observed laser ignition of HAN and HEHN propellant mixture. Recently, papers have been reported on the potential use of ILs as hypergols.**[6,7,14-16]**

*1.4. Chemical nature of vapor above ILs*

The chemical nature of the vapor above an ionic liquid is difficult to determine. It is, however, important to know how the vapor pressure forms from an ionic liquid because ignition occurs in the gas phase above the liquid. Experimental findings and theoretical calculations have been reported in the literature on this issue.**[17-23]** Ionic liquids can be divided into two classes: protic ionic liquids and aprotic ionic liquids. Protic ILs have hydrogen atoms on the ring nitrogens, whereas aprotic ILs have alkyl groups on the ring nitrogens instead of hydrogen atoms. For a protic ionic liquid abbreviated as $BH^+ X^-$, for instance, there could be ion pairs ($BH^+ X^-_{(g)}$), separated ions ($BH^+_{(g)} + X^-_{(g)}$), neutral pairs $BHX_{(g)}$ or separated neutrals ($B_{(g)} + HX_{(g)}$) in equilibrium above the liquid surface. Apparently, protic ILs only evaporate as separated neutrals **[23]** whereas many aprotic ILs evaporate as ion pairs.**[24]** For monopropellant systems where a single ionic liquid is heated up to ignition, a detailed understanding of the relative importance of these processes would be of significant importance to properly model the behavior. On the other hand, for room temperature ILs/WFNA mixtures, the gas-phase composition may be more complex because

exothermic reactions occurring in the liquid phase will produce additional gaseous species not observed above the pure ionic liquid. The concentrations of these additional species likely exceed that of the pure IL components, and may ultimately be responsible for the hypergolicity of the system.

## 2. Thermochemistry of compounds formed during IL-WFNA reactivity

The most important feature of the MMH/NTO system is its hypergolicity, which is its auto-ignition at ambient temperatures and pressures. Recently, hypergolic ionic liquids have been cited in the literature,**[6,7, 14-16]** which include mechanistic information on a class of ILs which exhibit hypergolicity at room temperature with WFNA. The proposed mechanism of the reactions in the liquid phase was used to explain the FTIR observations of the gas phase species above the reacting IL and WFNA mixtures. In the 1-butyl-3-methylimidazolium dicyanamide reaction with WFNA, gas-phase $HNO_3$, $CO_2$, $N_2O$, HNCO, $H_2O$, and $NO_2$ was observed prior to ignition. HNCO, $N_2O$ and $CO_2$ were presumably formed from dinitrobiuret,**[25]** $NO_2NHCONHCONHNO_2$ (abbreviated as DNB, Fig. 1), which decomposes thermally to give, intermediate #1, $NO_2NHCONCO$ (Fig. 1), and intermediate #2, $NH_2NO_2$ (Fig. 1) according to:

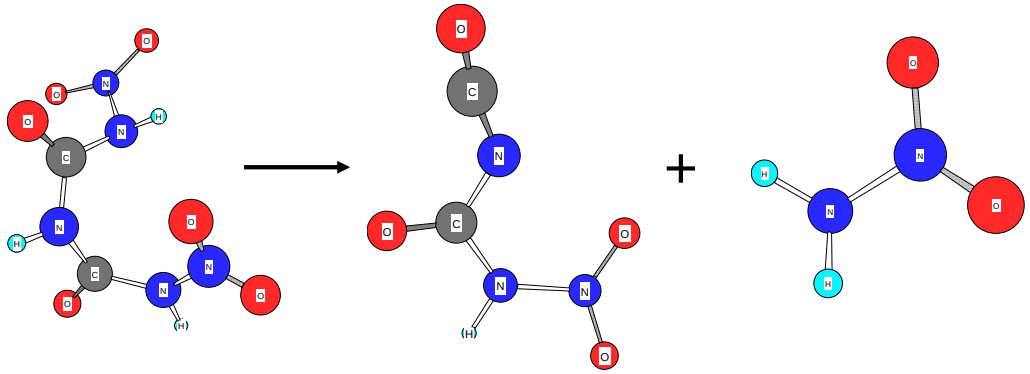

**Fig. 1: Thermal decomposition of DNB in the liquid phase leading to two condensed phase products; intermediates #1 and #2. The thermal decomposition of these products is considered to be the source of the species observed in the gas phase before ignition.**

The two intermediates in the liquid phase can decompose to give HNCO + $N_2O$ + $CO_2$, and $N_2O$ + $H_2O$, respectively. These compounds, together with $HNO_3$ and $NO_2$ from WFNA, are thought to lead to ignition. DNB and intermediates #1 and #2 were not observed in the gas phase. This is not surprising because DNB and the intermediates are highly reactive and therefore short-lived and are not likely to be detected. DNB is known to decompose around 373 K.**[25]** Here, we will attempt to explain the ignition by considering only those species actually observed in the gas phase. However, for completeness, the thermochemistries of DNB and the intermediates are also briefly discussed. DNB, intermediates #1 and #2 are nitro compounds and their gas-phase thermochemistries can be calculated by using the theoretical method previously established for nitro and nitrate compounds.**[26]** Thermodynamics data

(standard enthalpy of formation at 298 K, Cp° against T and S° against T) on these species are needed for further refinements of the derived gas-phase ignition models.

The gas-phase thermochemistry of DNB can be calculated by using a semi-empirical method established for nitro compounds. Validation of this method was presented by Osmont et al.**[22]** This procedure leads to a gas-phase standard enthalpy of formation of DNB at 298 K of -47.9 kcal $mol^{-1}$. For intermediate # 2, the nitramide molecule, the data available are somewhat inconsistent. Burcat and Ruscic **[27]** in the latest version of their thermodynamics database report two quite different values for the gas-phase standard enthalpy of formation at 298 K: -6.2±2.4 and -0.7±X.X kcal $mol^{-1}$. This method applied to $NH_2NO_2$ leads to +1.4±3.0 kcal $mol^{-1}$, which is more consistent with the second value reported above. Similarly, for intermediate #1, a value of -44.5±3.0 kcal $mol^{-1}$ is obtained. The enthalpy of the reaction DNB→#1+ #2 is +4.8 kcal $mol^{-1}$.

The main species in the gas phase above the reacting liquids are HNCO (isocyanic acid), nitric acid ($HNO_3$ or $HONO_2$), $NO_2$, $N_2O$, $H_2O$ and $CO_2$. The thermochemistries of these small species are generally known and are reported in the CHEMKIN format by Burcat and Ruscic.**[27]**

## 3. Detailed chemical kinetics model

### *3.1. Approach*

It seems clear, from the experimental studies presented in Section 2, that gaseous mixtures of HNCO, $HNO_3$, $N_2O$, $NO_2$, $CO_2$ and $H_2O$ are able to sustain a flame. However, the chemical pathways involved in ignition need to be elucidated, as they are critical to the detailed construction of a chemical kinetics model. Generally, detailed chemical kinetics models are validated with experimental data obtained with premixed mixtures at known temperatures and pressures, which include ignition delays, species profiles, fundamental flame speeds, etc. obtained under "ideal" laboratory setups. In the case of hypergolic systems, as is the case here, it is much more difficult to determine the exact composition, pressure and temperature of the gas phase prior to ignition and therefore will be much more difficult to validate a given chemical kinetics model. The approach followed here consists of building a detailed chemical kinetics model (Section 3.3), followed by its validation with relevant experimental data published in the literature (Section 3.4). Once validated, the model is then used to interpret the main features of the hypergolic ignition studied in this work through various sensitivity analyses (Section 3.5).

*3.2. Mixtures under consideration*

By considering the equations given in Ref. 14, for one mole of DNB decomposed in the liquid phase, there will be an equal amount of HNCO, $CO_2$, $H_2O$ and twice this amount of $N_2O$ in the gas phase. $N_2O$ is known not only as an oxidant but also as a monergol, that is, its decomposition is so exothermic that it can sustain a decomposition flame. The amount of gas-phase $HNO_3$, at a given temperature, will depend on the type of liquid solution formed with IL and WFNA; either an ideal solution, in which case, Raoult's law will be followed, or a non-ideal solution, for which, the values of the activity coefficients of the species would be needed. Furthermore, here the reacting liquid mixture is inhomogeneous in nature.

Moreover, a small amount of $NO_2$ can be present in the WFNA. Therefore, in the mixtures under consideration here, there is one type of fuel molecule (HNCO), three types of oxidizer molecules ($HNO_3$, $NO_2$ and $N_2O$), and two types of almost unreactive species ($H_2O$ and $CO_2$) prior to ignition. Since the quantitative composition is not known, various mixtures need to be considered parametrically in the kinetics model simulations such as: 1 HNCO/ 1 $CO_2$ / 1 $H_2O$ / 2 $N_2O$ / $\alpha$ $HNO_3$ / 0.01 $NO_2$, with $0.1 < \alpha < 2$.

*3.3. Building of a detailed chemical kinetics model*

Dagaut et al.**[28]** have published a detailed kinetics model of HCN oxidation (with 41 species and 250 reactions) in which an HNCO sub-mechanism has been considered. Their HNCO and $HONO_2$ sub-mechanisms were rather limited, therefore, here additional reactions have been added to the Dagaut et al. model. Also, for completeness, the C-species sub-model has been included, although its impact to the ignition modeling of HNCO is expected to be minimal as it is for HCN oxidation. Thermal decompositions of all the reactants (HNCO, $HNO_3$, etc.) are also explicitly considered. The detailed chemical kinetics model written for this work contains 70 species and 506 reactions. This model is reported as supplementary information. Rate coefficients employed are from various literature sources.**[28-30]** It is to be noted that the reaction kinetics of some of the steps of isocyanic acid (HNCO) decomposition and oxidation in the gas phase have previously been extensively studied because HNCO is the decomposition product of cyanuric acid, which is the prime reagent of the RapreNOx process for $NO_x$ removal.**[29]** However, despite these studies, no detailed kinetics model has been specifically devoted to HNCO and validated with all of the available experimental data in the literature, and this work attempts to bridge this gap in our model.

*3.4. Validation of the detailed chemical kinetics model*

The CHEMKIN-II **[31]** and SENKIN **[32]** codes were used to integrate the time-dependent rate equations derived from the reaction mechanism. Direct experimental data reported in the literature concerning various HNCO-based systems, such as HNCO/Ar, HNCO/$N_2O$/Ar, and HNCO/$NO_2$/Ar are considered here. These data were not considered in the HNCO submechanism by Dagaut et al.**[28]** for the validation of their HCN oxidation kinetics model, which was instead validated with available data on HCN-based systems such as HCN/$HNO_3$/Ar and HCN/$O_2$/Ar. For model validation purposes, comparisons between experimental data and predictions of the models are reported in Figs. 2-6 for HCN-based systems. As shown in these figures, our expanded model results in little changes to Dagaut's predictions for HCN-based systems.

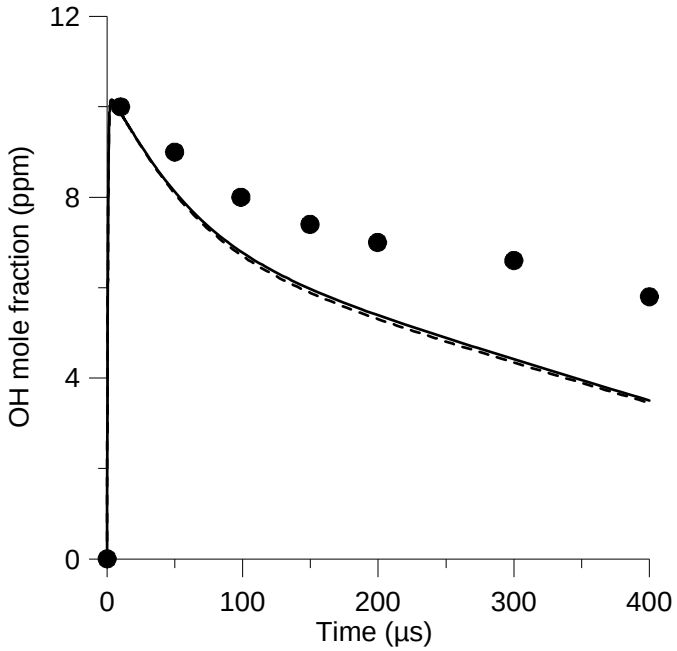


**Fig. 2: Calculated and experimental OH profiles for the mixture; 10.3 ppm $HNO_3$ + 0.34% HCN in Ar, T = 1492 K and P = 1.01 atm. Points are experimental values (as reported in Ref. 28), solid line is from present model and dashed-line is from Ref. 28.**

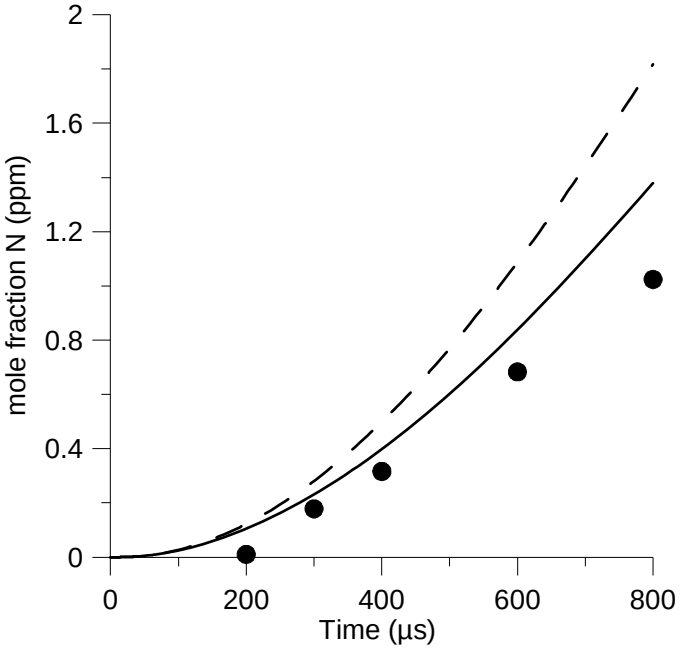


**Fig. 3: Calculated and experimental N profiles for the mixture; 50 ppm HCN + 50 ppm $O_2$ in Ar, T = 2600 K and P = 1.78 atm. Points are experimental values (as reported in Ref. 28), solid line is from present model and dashed-line is from Ref. 28.**

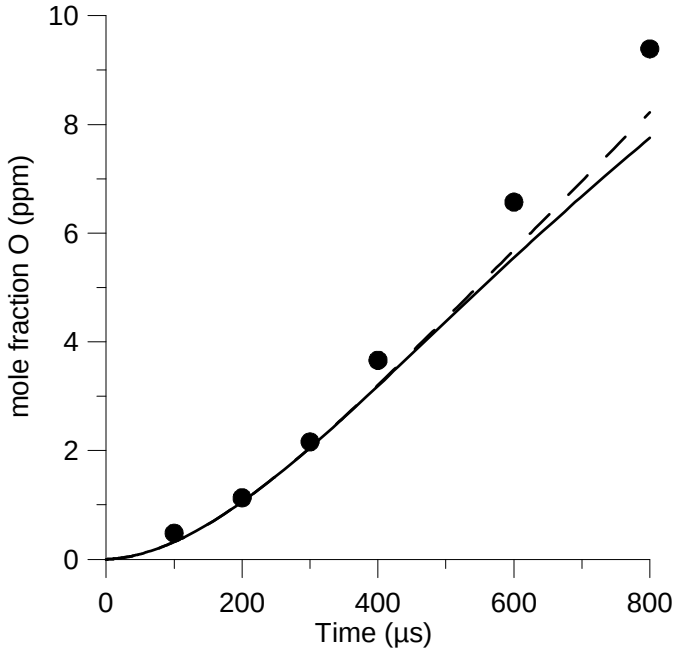

**Fig. 4: Calculated and experimental O profiles for the mixture; 50 ppm HCN + 50 ppm $O_2$ in Ar, T = 2826 K and P = 1.69 atm. Points are experimental values (as reported in Ref. 28), solid line is from present model and dashed-line is from Ref. 28.**

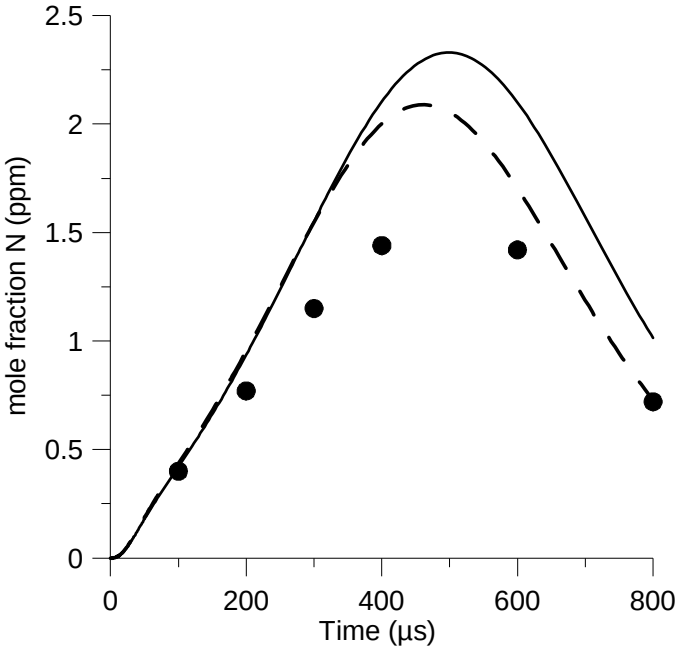


**Fig. 5: Calculated and experimental N profiles for the mixture; 100 ppm HCN + 1000 ppm $O_2$ in Ar, T = 2718 K and P=1.78 atm. Points are experimental values (as reported in Ref. 28), solid line is from present model and dashed-line is from Ref. 28.**

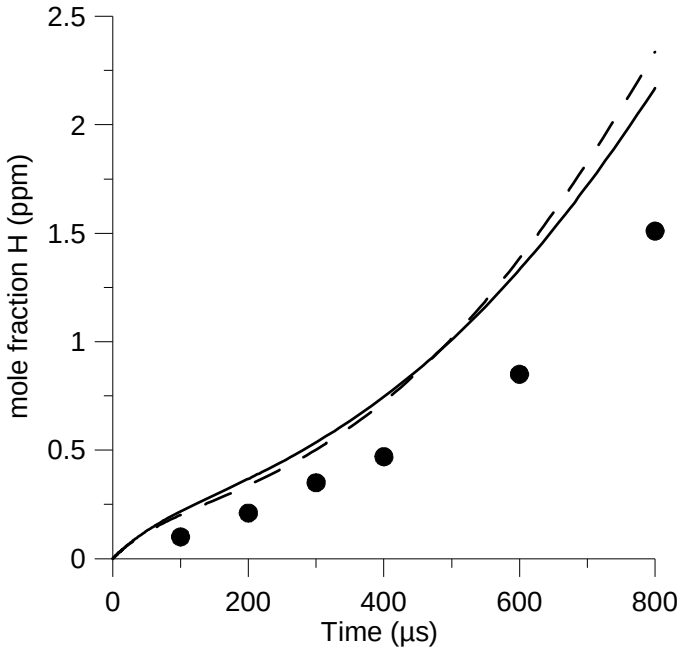


**Fig. 6: Calculated and experimental H profiles for the mixture; 50 ppm HCN + 250 ppm $O_2$, T = 2625 K and P = 1.82 atm. Points are experimental values (as reported in Ref. 28), solid line is from present model and dashed-line is from Ref. 28.**

More importantly, this expanded model considers the low temperature (673-773 K) data that are available for HNCO/$NO_2$/Ar mixtures.**[30]** The temperature reached in the gas phase when hypergolic ignition occurs is estimated to be about 423 K and therefore these relatively low temperature data are particularly important for the validation of the present detailed chemical kinetics model and for its predictive ability at around 423 K. However, this temperature range was beyond the scope of Dagaut et al. study and almost all of the data they considered were obtained at 900 K or above. The Dagaut et al. model does not correctly predict the HNCO/$NO_2$ reactivity in the 673-773 K temperature range (Figure 7), whereas this model comes much closer to predicting the experimental HNCO mole fraction by using the rate coefficients recommended by He et al.**[30]**

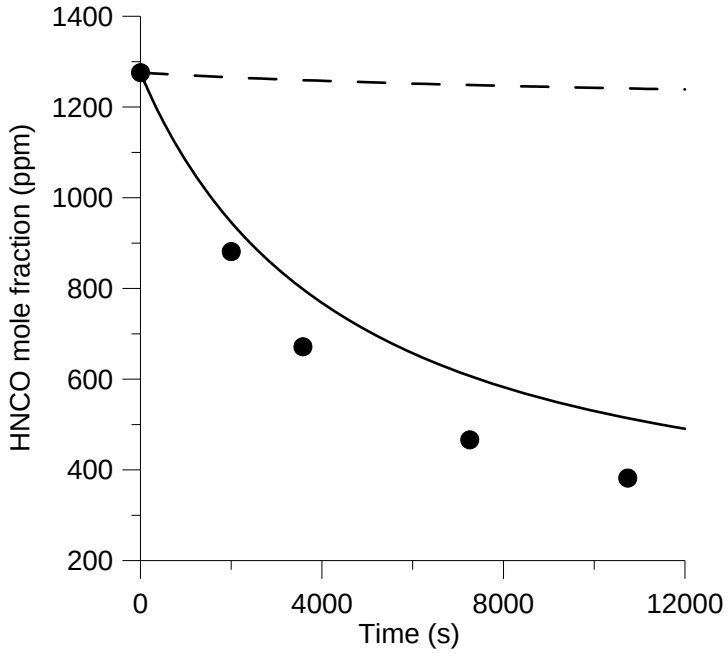


**Fig. 7: Calculated and experimental HNCO profiles for the mixture; 1275.84 ppm HNCO + 1485.68 ppm $NO_2$ in Ar, T = 673 K and P = 0.658 atm. Points are experimental values of Ref. 30, solid line is from present model and dashed-line is from Ref. 28.**

The predictions of the present model are compared to low temperature species profiles obtained in a static reactor (Figs. 8a-f).**[30]** Experimental data and predicted data agree well for all the species profiles except for $CO_2$ whose formation is generally over predicted. However, experimental data and predicted data remain within a factor 2.

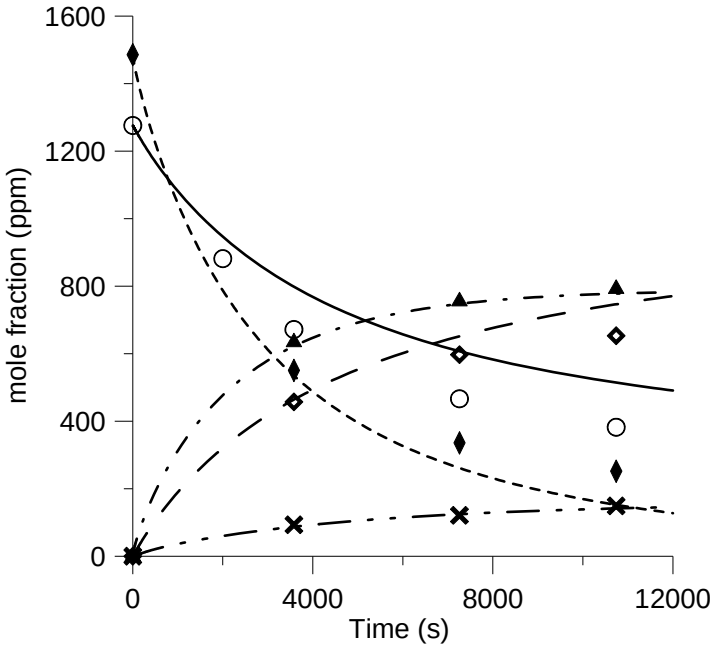


**Fig. 8a: Experimental points (from Ref. 30) and calculated curves (present model) for NO (▲ and - · - · - · - ·), $CO_2$ (◇ and – – – – ), HNCO (○ and ————), $N_2O$ (✕ and – · · – · · –), and $NO_2$ (♦ and .....) for the mixture; 1275.84 ppm HNCO + 1485.68 ppm $NO_2$ in Ar, T = 673 K and P = 0.658 atm.**

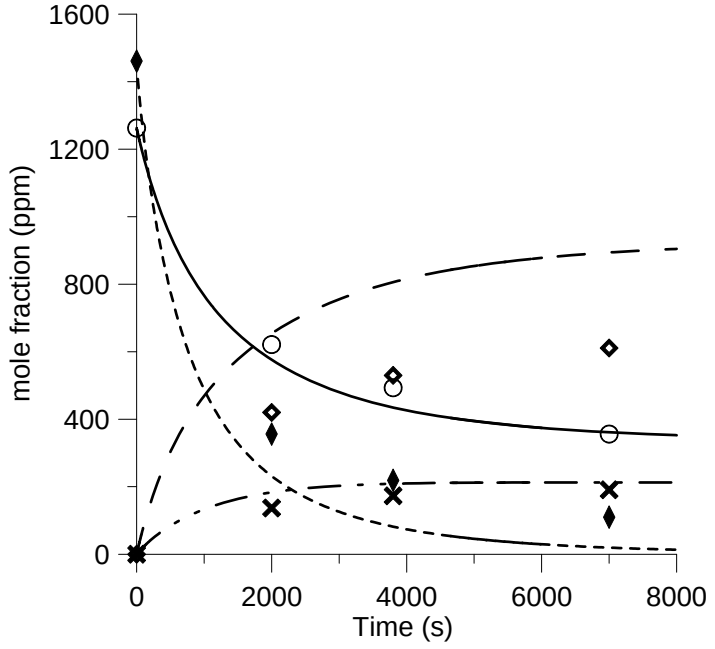


**Fig. 8b: Experimental points (from Ref. 30) and calculated curves (present model) for $CO_2$ (◇ and – – – – ), HNCO (○ and ————), $N_2O$ (✕ and – · · – · · –), and $NO_2$**

**(♦and .....) for the mixture; 1262.4 ppm HNCO + 1460.8 ppm $NO_2$ in Ar, T = 723 K and P = 0.658 atm.**

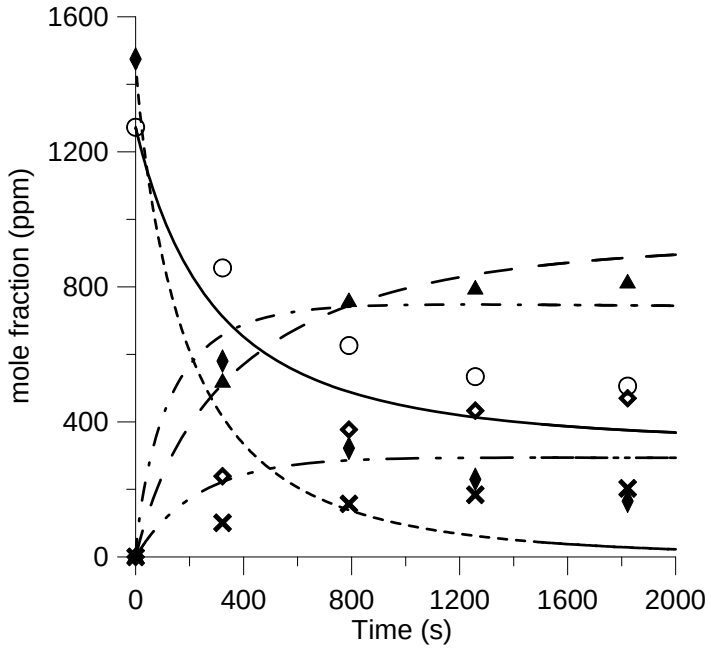


**Fig. 8c: Experimental points (from Ref. 30) and calculated curves (present model) for NO (▲ and - - - - - -), $CO_2$ (◇ and – – – – ), HNCO (○ and ————), $N_2O$ (✕ and – . . – . . –), and $NO_2$ (♦and .....) for the mixture; 1272.6 ppm HNCO + 1475 ppm $NO_2$ in Ar, T = 773 K and P = 0.658 atm.**

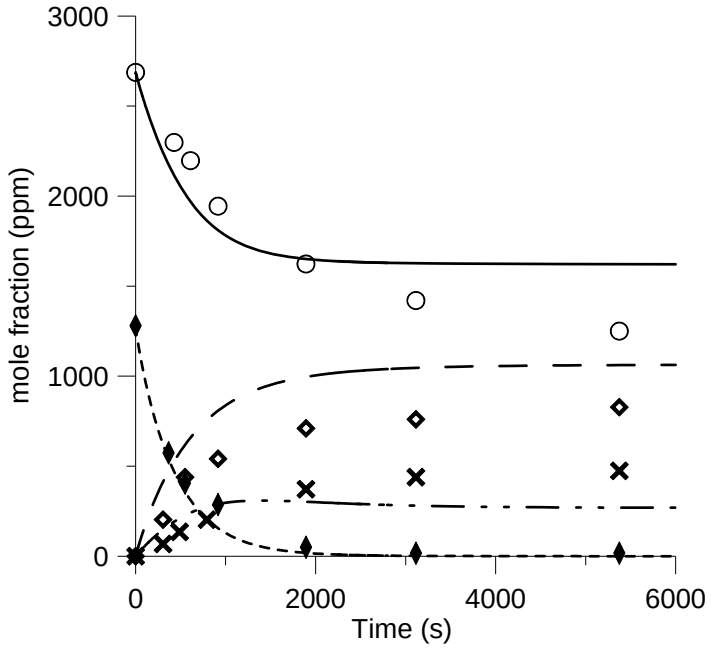


**Fig. 8d: Experimental points (from Ref. 30) and calculated curves (present model) for $CO_2$ (◇ and ▬ ▬ ▬ ▬ ), HNCO (○ and ▬▬▬▬), $N_2O$ (✕ and ▬ · · ▬ · · ▬), and $NO_2$ (⧫ and .....) for the mixture; 2687 ppm HNCO + 1280 ppm $NO_2$, T = 723 K and P = 0.658 atm.**

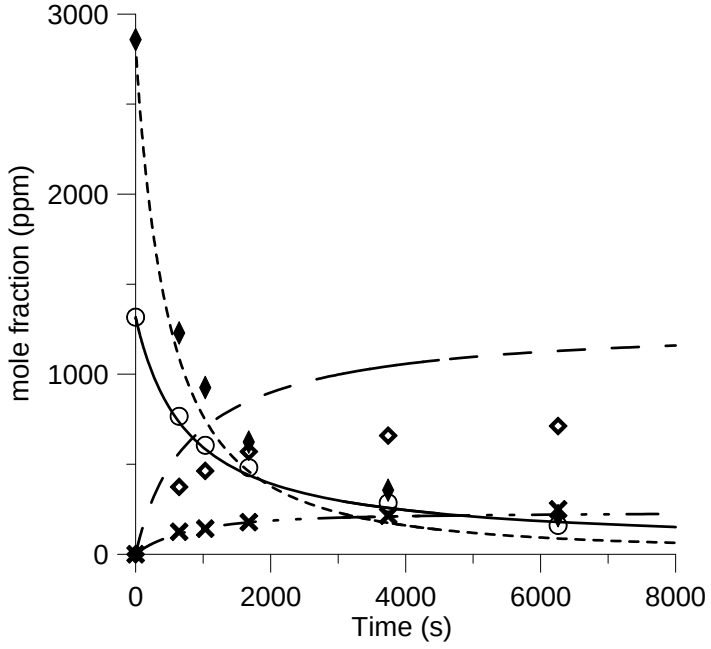


**Fig. 8e: Experimental points (from Ref. 30) and calculated curves (present model) for $CO_2$ (◇ and ▬ ▬ ▬ ▬ ), HNCO (○ and ▬▬▬▬), $N_2O$ (✕ and ▬ · · ▬ · · ▬), and $NO_2$**

**(♦and .....) for the mixture; 1316.5 ppm HNCO + 2858.4 ppm $NO_2$, T = 723 K and P = 0.658 atm.**

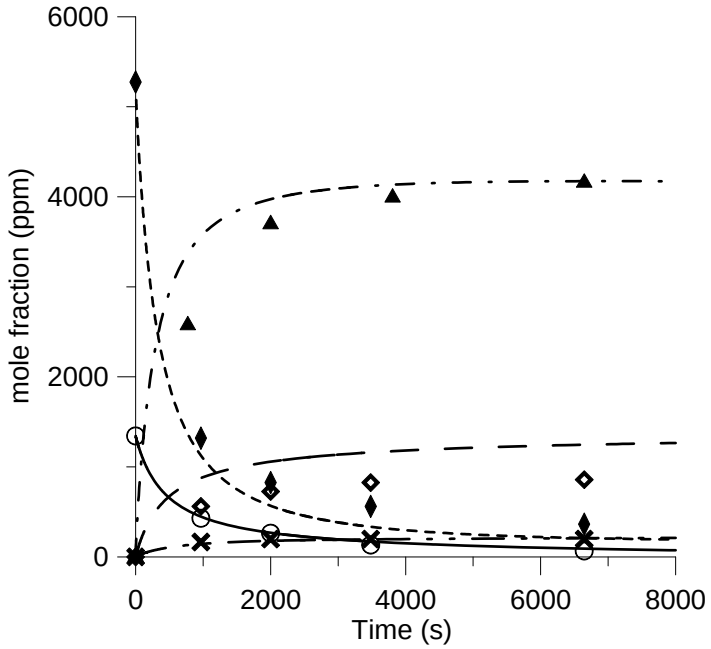


**Fig. 8f: Experimental points (from Ref. 30) and calculated curves (present model) for NO (▲ and - - - - - -), $CO_2$ (◇ and — — — — ), HNCO (○ and ————), $N_2O$ (✕ and — · · — · · —), $NO_2$ (♦and .....) for the mixture; 1343.5 ppm HNCO + 5274.8 ppm $NO_2$ in Ar, T = 723 K and P = 0.658 atm.**

The present study is devoted to hypergolic ignition chemistry which occurs at ambient or relatively low temperatures. However, for completeness, high-temperature data above 1000 K have also been considered. The agreement between experiments and calculations is good for almost all of the experimental data,**[28, 33-36]** whatever the system studied, and whatever the temperature and pressure range employed. In particular, as shown in Figs. 9a-9d, the NCO profiles at high temperature are generally better predicted with the present model than with the model of Dagaut et al.**[28]** This is very important because the amounts of NCO produced are generally quantitatively important on the order of hundreds of ppm.

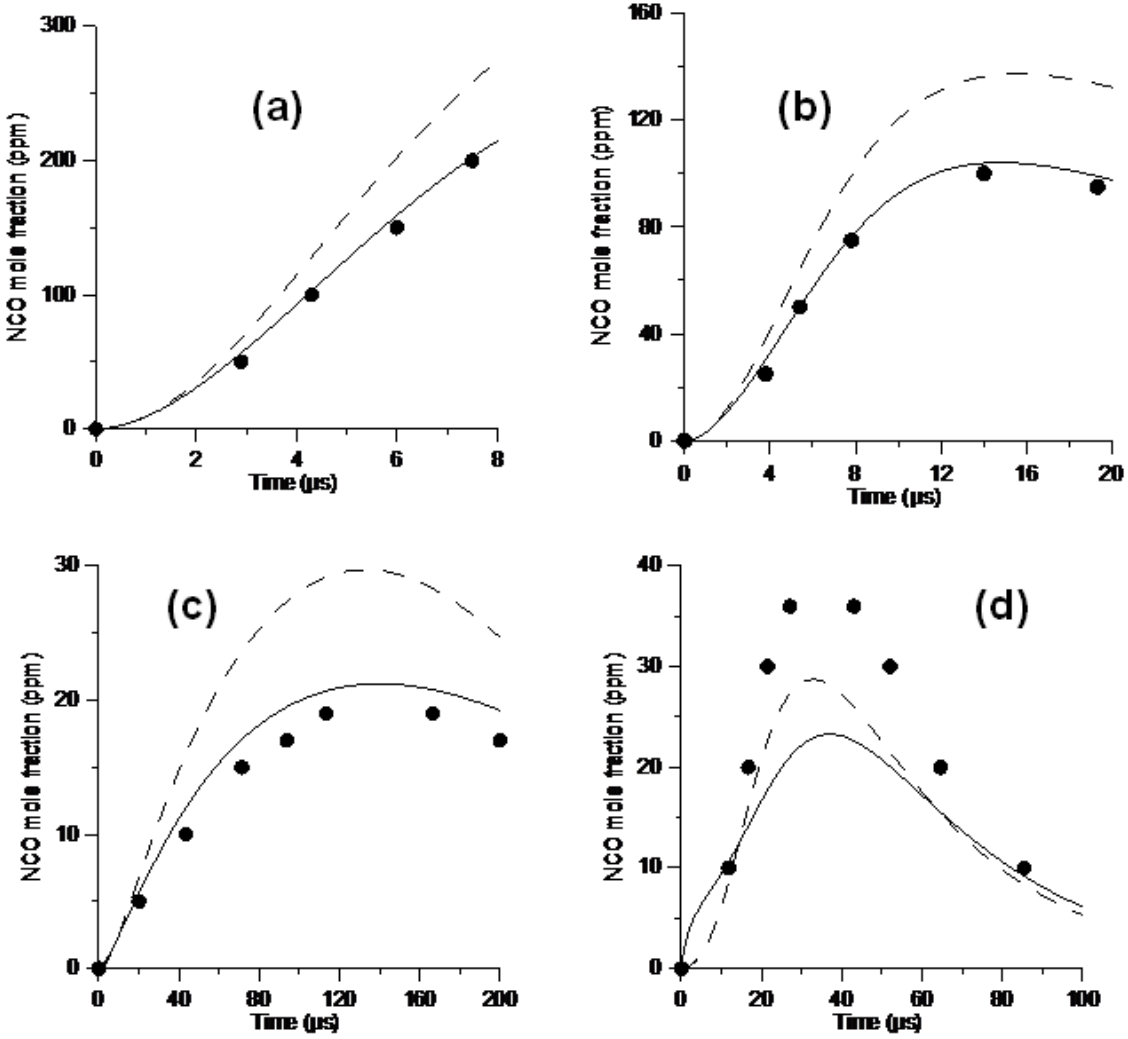


**Fig. 9**: Calculated and experimental NCO profiles for the mixtures: **a)** 1 mol% HNCO + 1 mol% $N_2O$ in Ar, T = 2380 K and P = 1.07 atm. **b)** 0.3 mol% HNCO + 1 mol% $N_2O$ in Ar, T = 2380 K and P = 1.14 atm. **c)** 0.3 mol% HNCO + 1.5 mol% NO in Ar, T = 2383 K and P = 1.12 atm. **d)** 0.2 mol% HNCO in Ar, T = 2920 K and P = 0.92 atm. Points are experimental values of Ref. 33, solid line is from present model and dashed-line is from Ref. 28.

In contrast, the NH profiles are generally better predicted when using the model of Dagaut et al. (Fig. 10a) but it is not always the case (Fig. 10b). However, the amounts of NH are rather low, 10 ppm at most, and predictions using the present model are still within a factor of 2.

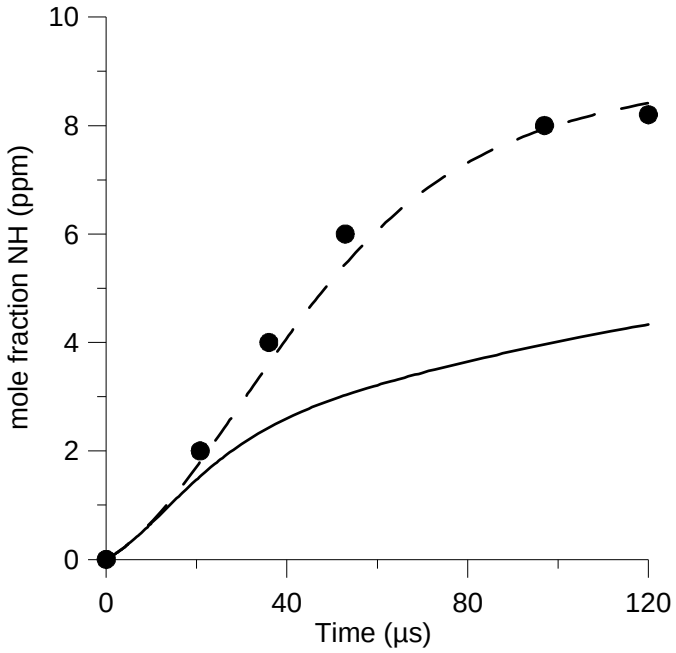


**Fig. 10a: Calculated and experimental NH profiles for the mixture, 0.1 mol% HNCO + 0.24 mol% $N_2O$ in Ar, T = 2175 K and P = 0.336 atm. Points are experimental values of Ref. 35, solid line is from present model and dashed-line is from Ref. 28.**

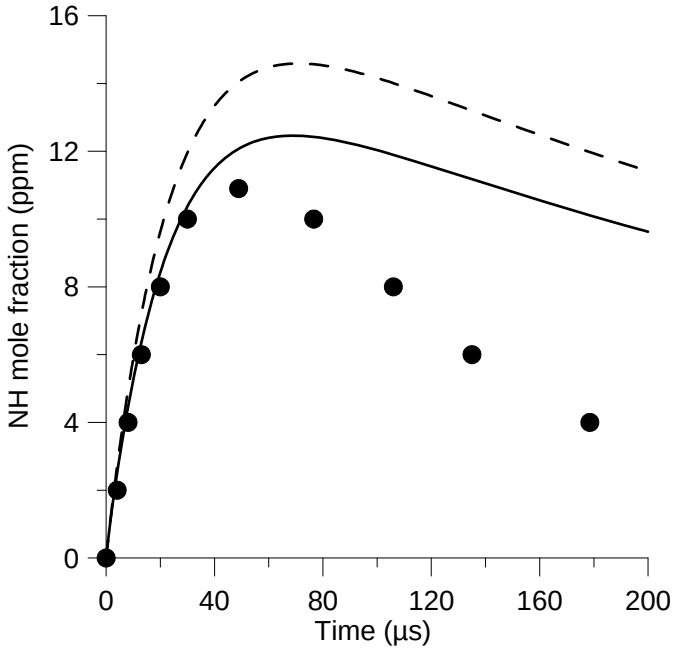

**Fig. 10b: Calculated and experimental NH profiles for the mixture: 17 ppm HNCO in Ar, T = 3186 K and P = 0.805 atm. Points are experimental values of Ref. 36, solid line is from present model and dashed-line is from Ref. 28.**

For OH radicals, as shown in Fig. 11, both models predict similar profiles and are in agreement with the experimental data.

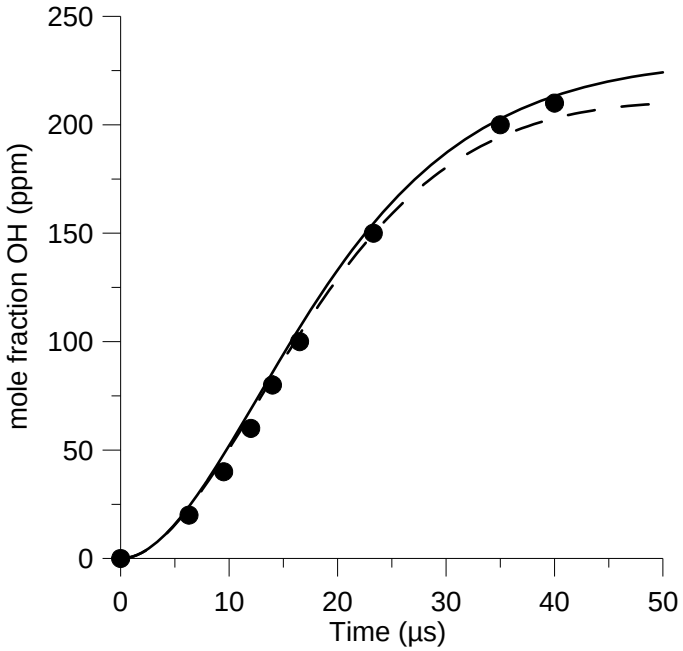


**Fig. 11: Calculated and experimental OH profiles for the mixture: 0.5 mol% HNCO + 0.25 mol% $N_2O$ in Ar, T = 2555 K and P = 0.505 atm. Points are experimental values of Ref. 35, solid line is from present model and dashed-line is from Ref. 28.**

The occasional disagreement observed at high temperatures suggests further refinements and studies are needed, and reassessment of some of the rate coefficients used.

*3.5. Predictions of the kinetics model*

The full kinetics model with reaction **R506** shown below but not originally considered, was used to predict the fate of premixed gas mixtures; 1 HNCO/ 1 $CO_2$ / 1 $H_2O$ / 2 $N_2O$/ α $HNO_3$/

0.01 $NO_2$ with $0.1 < \alpha < 2$ at initially 423 K and 1 atm, as well as examine the ignition delays. The model is able to simulate ignition at the relatively low temperature of 423 K. However, computed ignition delay times are longer by several orders of magnitude compared to reported experimental values.**[14,16]** The cause of this is unlikely to be erroneous extrapolations of the rate coefficients to 423 K because the model is reasonably predictive in the wide 673-3186 K temperature range. Therefore, additional reactions need to be included in the model. Wooldridge et al. reported that isocyanic acid and nitric acid react at room temperature to form $CO_2$, $H_2O$ and $N_2O$.**[37]**

$$H\text{-}N{=}C{=}O + HO\text{-}NO_2 \rightarrow CO_2 + H_2O + N_2O \qquad (\mathbf{R506})$$

The reaction probably proceeds via $O_2N$-N=C=O formation and $H_2O$ elimination, with the former rapidly decomposing to give $CO_2$ and $N_2O$. The above global reaction was thus incorporated into the kinetics model with a rate coefficient value sufficiently high to compute ignition delay times that were comparable to experimentally observed values, but sufficiently low to have no influence on the reported predictions of Figs 2-11. For example, ignition delay times $\tau$ of ~700 ms at constant volume and of ~2 s at constant pressure for $\alpha = 1$ were computed (see Table 1 and Fig. 12). No additional reactions seem to explain this feature.

| $\alpha$ | $\tau$ (s) at constant volume | $\tau$ (s) at constant pressure |
|---|---|---|
| 0.05 | No ignition | No ignition |
| 0.1 | No ignition | No ignition |
| 0.2 | 2500 | No ignition |
| 0.3 | 9 | 275 |
| 0.4 | 2 | 12 |

| | | |
|---|---|---|
| 0.5 | 1.2 | 4 |
| 0.6 | 1 | 3 |
| 0.7 | 0.8 | 2 |
| 0.8 | 0.8 | 2 |
| 0.9 | 0.75 | 2 |
| 1 | 0.7 | 2 |
| 1.5 | 0.8 | 3 |

**Table 1. Calculated ignition delays τ at constant pressure, and at constant volume for the mixtures; 1 HNCO/ 1 $CO_2$ / 1 $H_2O$ / 2 $N_2O$/ α $HNO_3$/ 0.01 $NO_2$ with 0.05 < α < 1.5 initially at 423 K and 1 atm.**

In Table 1, from $\alpha = 1$ to $\alpha = 1.5$, $\tau$ begins to increase with increasing $HNO_3$ concentration because here the excess $HNO_3$ does not play the role of an oxidizer but of a diluent which inhibits the reaction, not chemically but physically by absorbing part of the exothermicity.

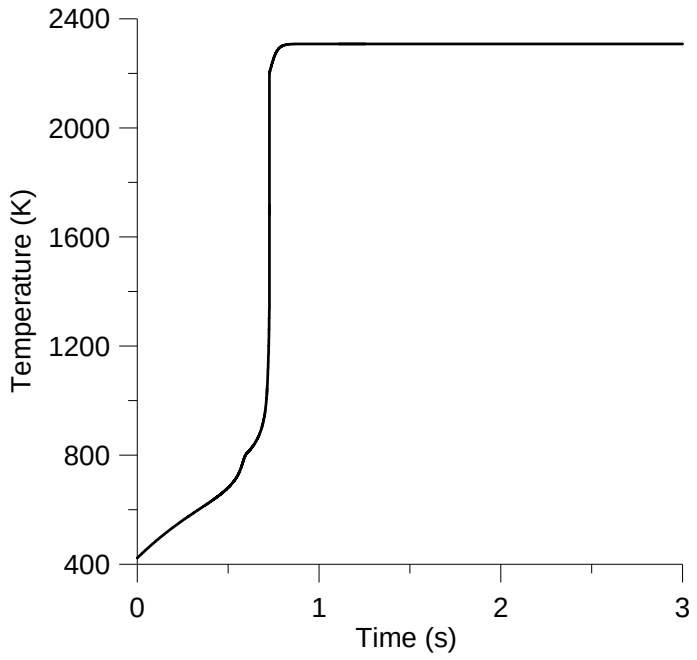


**Fig. 12: Computed temperature profile for the mixture, HNCO/$NO_2$/$N_2O$/$CO_2$/$H_2O$/$HNO_3$: 1/0.01/2/1/1/1. The system is assumed to be adiabatic and at constant volume. P = 1 atm and T = 423 K. Ignition delay τ is 730 millisecond.**

*3.6. Summary of gas-phase $HNCO/HONO_3/N_2O/H_2O/CO_2/NO_2$ chemistry*

Sensitivity analyses, performed with the full kinetics model, enable the identification of redundant species and reactions, that is, species and reactions that do not affect the flow of the reaction system. Several sensitivity analyses exist. In the method of brute force sensitivity analysis, the kinetics code is run by perturbing one parameter and comparing the results to the original unperturbed model. For instance, a rate coefficient can be set equal to zero (as if to remove the reaction from the system) and see if the reaction is important in the process. In another approach, the value of the rate coefficient of a reaction may be multiplied or divided generally between two and five to ascertain its importance in the model. Modification of the rate coefficient of an important reaction will induce relatively large variations in the predicted ignition delay. Such sensitivity analyses were performed for the representative mixture in Fig. 12 during pre-ignition from time zero to ~700 ms. Together with these sensitivity analyses, local sensitivity analyses (as implemented in CHEMKIN-II), for several species not reported here and for the temperature were performed. The normalized sensitivity coefficient, $\omega_j$, for temperature is defined as:

$$\omega_j = \left( \frac{\partial T}{\partial A_j} \right) \frac{A_j}{T}$$

with j as the index of the reaction and $A_j$ as the pre-exponential factor of its reaction rate coefficient. Essentially, $\omega_j$ is a measure of how the system temperature depends upon $A_j$, where a positive $\omega_j$ indicates an increase in system temperature with an increase in the reaction pre-exponential factor, and a negative $\omega_j$ indicates a decrease in system temperature with increasing reaction pre-exponential factor. From these sensitivity studies, the gas-phase

chemistry can be summarized as in Fig. 13. Reaction 506 (hereafter noted as **R506**) shows the most sensitive in the model even at the shortest times and lowest temperatures. The exothermicity of **R506** (H-N=C=O + HO-$NO_2$ → $CO_2$ + $H_2O$ + $N_2O$) induces significant thermal decomposition of nitric acid according to -**R210**:

$$HONO_2 (+M) \rightarrow NO_2 + OH (+M) \qquad (\textbf{-R210})$$

The OH and $NO_2$ chain carriers may then react according to:

$$HNCO + OH \rightarrow NCO + H_2O \qquad (\textbf{R40})$$

$$HONO_2 + OH \rightarrow H_2O + NO_3 \qquad (\textbf{R475})$$

$$NO + OH (+M) \rightarrow HONO (+M) \qquad (\textbf{R164})$$

$$NO_2 + OH \rightarrow NO + HO_2 \qquad (\textbf{R165})$$

and

$$HNO + NO_2 \rightarrow HONO + NO \qquad (\textbf{R153})$$

$$NCO + NO_2 \rightarrow CO + 2NO \qquad (\textbf{R70})$$

NCO radicals, mostly formed by **R40**, also react with $NO_2$ according to:

$$NCO + NO_2 \rightarrow CO_2 + N_2O \qquad (\textbf{R71})$$

This reaction is highly exothermic (~500 kJ $mol^{-1}$) and could be expected to play an important role in the ignition process. However, this expectation is not realized because model does not appear to be very sensitive to it shown Fig. 13.

NO, formed by **R153**, **R70** and **R165**, reacts with $NO_3$ according to:

$$NO + NO_3 \rightarrow NO_2 + NO_2 \qquad (\textbf{-R178})$$

where the $NO_3$ is formed in **R475** as well as in **R505**.

$$HNNO + NO_2 \rightarrow NNH + NO_3 \qquad (\textbf{R505})$$

The HNO radicals reacting in **R153** are mostly formed by:

$$HNCO + NO_3 \rightarrow CO_2 + NO + HNO \qquad (\textbf{R479})$$

$$HNNO + NO_2 \rightarrow HNO + NO + NO \qquad (\textbf{-R490})$$

HNNO species reacting in **R505** and **-R490** are formed by:

$$HNCO + NO_2 \rightarrow CO_2 + HNNO \qquad (\textbf{R480})$$

$HO_2$ is formed by reaction **R165** and reacts according to **R175**:

$$NO_2 + HO_2 \rightarrow HONO + O_2 \qquad (\textbf{R175})$$

$H_2O$ and $N_2O$, which are initially present, do not react during the ignition delay period because of the low temperatures but are respectively formed by **R506** and **R475**, and by **R506** and **R71**.

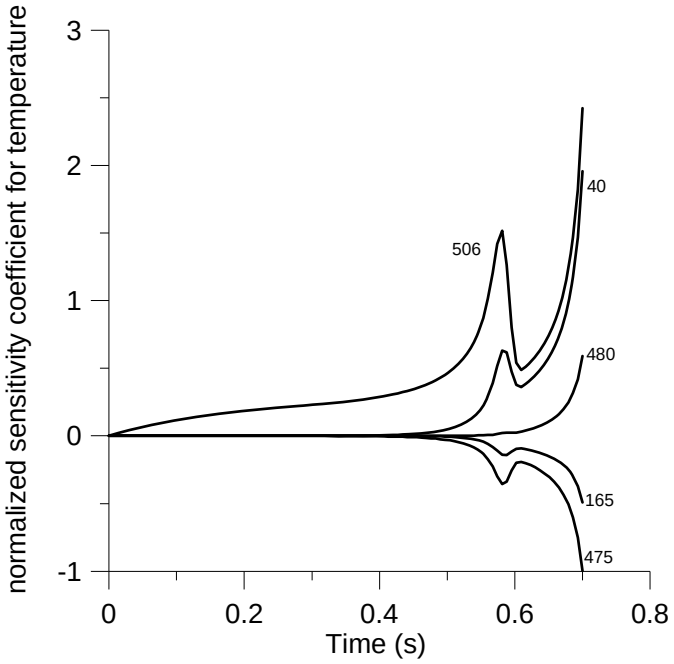


**Fig. 13: Sensitivity plot for temperature for the five most sensitive reactions: (R506) H-N=C=O + HO-$NO_2$ → $CO_2$ + $H_2O$ + $N_2O$, (R40) HNCO + OH → NCO + $H_2O$, (R480) HNCO + $NO_2$ → $CO_2$ + HNNO, (R165) NO + $HO_2$ → $NO_2$ + OH and (R475) $HONO_2$ + OH → $H_2O$ + $NO_3$.**

Fig. 14 shows the model's fidelity in predicting the ignition delay time when **R506** rate coefficient value is doubled and when it is halved. The predicted ignition delay values are ~ 350 ms and 1400 ms. Other reactions are less influential on the predicted ignition delays. This further indicates the importance of **R506**.

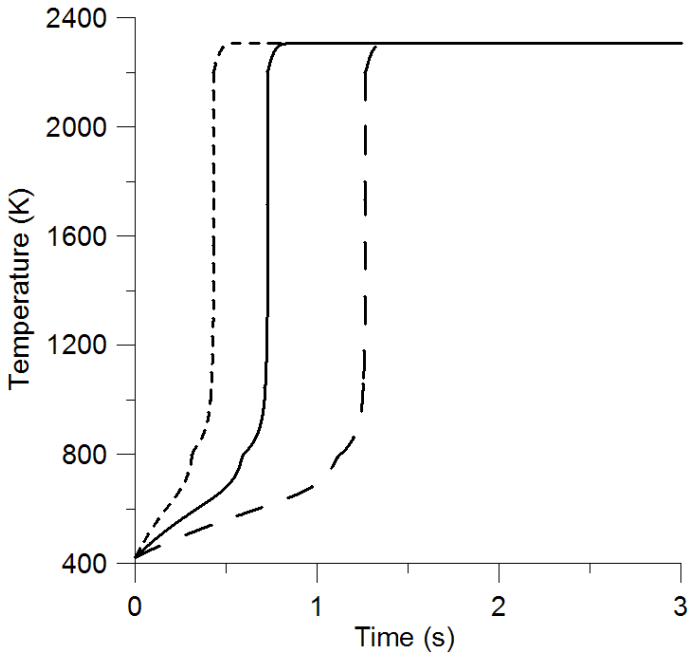


**Fig. 14: Brute-force sensitivity analysis. Comparison between calculated ignition delays with variation of the rate coefficient for R506. Solid line: present model. Dotted line: pre-exponential factor multiplied by 2. Dashed line: pre-exponential factor divided by 2.**

## 4. Conclusions

Experimentally demonstrated hypergolicity between an ionic liquid (IL) and nitric acid has been interpreted here by using a detailed chemical kinetics model. An exothermic reaction between isocyanic acid and nitric acid needs to be considered in the model to explain ignition. The full kinetics model is shown to be valid in a wide temperature range (673-3186 K). Various sensitivity analyses show that this exothermicity induces the thermal decomposition of some of the unreacted nitric acid to generate OH and $NO_2$, which then act as chain carriers up to autoignition. Several other reactions, important below 1000 K, have also been added in the present model. The present full model with 70 species and 506 reactions can be cast into a reduced form and still capture accurately the overall chemical description of the ignition process. Reduced forms often can eliminate ~ 90% of the original reactions from the full model and this can allow for the implementation of chemistry into computational codes which

deal with the physics of hypergolicity (i.e., fluid mechanical and thermal transfer effects). It appears from the results of the present study that the published chemical kinetics model of HNCO oxidation needs to be further investigated, and that reappraisal of some of the rate coefficients will probably be necessary.

## 5. Acknowledgments

This research was supported by the European Office of Aerospace Research & Development (EOARD) under contract # FA8655-07-M-4009 and by the Air Force Office of Scientific Research (AFOSR) under contract # FA9300-06-C-0023.

## 6. References

[1] L. Catoire, N. Chaumeix, C. Paillard, J. Prop. Power 20 (2004) 87-92.

[2] L. Catoire, N. Chaumeix, C. Paillard, J. Prop. Power 22 (2006) 120-126.

[3] S. Pichon, L. Catoire, N. Chaumeix, C. Paillard, J. Prop. Power, 21 (2005) 1057-1061.

[4] A. Osmont, L. Catoire, T.M. Klapötke, G.L. Vaghjiani, M.T. Swihart, Propellants Explosives Pyrotechnics 33 (2008) 209-212.

[5] Y. Ishikawa, M.J. McQuaid, J. Molecul. Structure: THEOCHEM 818 (2007) 119-124.

[6] Y. Zhang, J.M. Shreeve, Angewandte Chemie Int. Ed. 50 (2011) 935-937.

[7] L. He, G.-H. Tao, D.A. Parrish, J.M. Shreeve, Chemistry – A European Journal 16 (2010) 5736-5743.

[8] S. Trohalaki, R. Pachter, G.W. Drake, T. Hawkins, Energy & Fuels 19 (2005) 279-284.

[9] J.M.S.S Esperança, J.N.C. Lopez, M. Tariq, L.M.N.B.F. Santos, J.W. Magee, L.P.N. Rebelo, J. Chem. Eng. Data 55 (2010) 3-12.

[10] M. Smiglak, A. Metlen, R.D. Rogers, Acc. Chem. Res. 40 (2007) 1182-1192.

[11] C. Bigler Jones, R. Haiges, T. Schroer, K. O. Christe, Angew. Chem. Int. Ed. 45 (2006) 4981-4984.

[12] J. Li, T.A. Litzinger, Thermochimica Acta 454 (2007) 116-127.

[13] A.J. Alfano, J.D. Mills, G.L. Vaghjiani, Combustion Science and Technology 181 (2009) 902-913.

[14] S.D. Chambreau, S. Schneider, M. Rosander, T. Hawkins, C. Gallegos, M. Pastewait, G.L. Vaghjiani, J. Phys. Chem. A 112 (2008) 7816-7824.

[15] S. Schneider, T. Hawkins, M. Rosander, J. Mills, G.L. Vaghjiani, S.D. Chambreau, Inorganic Chemistry 47 (2008) 6082-6089.

[16] S. Schneider, T. Hawkins, M. Rosander, G.L. Vaghjiani, S.D. Chambreau, G. Drake, Energy & Fuels 22 (2008) 2871-2872.

[17] J.P. Armstrong, C. Hurst, R.G. Jones, P. Licence, K.R.J. Lovelock, C.J. Satterley, I.J. Villar-Garcia, Phys. Chem. Chem. Phys. 9 (2007) 982-990.

[18] K.J. Baranyai, G.B. Deacon, D.R. MacFarlane, J.M. Pringle, J.L. Scott, Aus. J. Chem. 57 (2004) 145-147.

[19] M.J. Earle, J.M.S.S. Esperança, M.A. Gilea, J.N. Canongia Lopes, L.P.N. Rebelo, J.W. Magee, K.R. Seddon, J.A. Widegren, Nature 439 (2006) 831-834.

[20] M.W. Schmidt, M.S. Gordon, J.A. Boatz, J. Phys. Chem. A 109 (2005) 7285-7295.

[21] D.D. Zorn, J.A. Boatz, M.S. Gordon, J. Phys. Chem. B 110 (2006) 11110-11119.

[22] V.N; Emel'yanenko, S.P. Verevkin, A. Heintz, J. Am. Chem. Soc. 129 (2007) 3930-3937.

[23] J.P. Leal, J.M.S.S. Esperança, M.E. Minas da Piedade, J.N. Canongia Lopes, L.P.N. Rebelo, K.R. Seddon, J. Phys. Chem. A 111 (2007) 6176-6182.

[24] D. Strasser, F. Goulay, M.S. Kelkar, E.J. Maginn, S.R. Leone, J. Phys. Chem. A 111 (2007) 3191-3195.

[25] J. Geith, G. Holl, T.M. Klapötke, J.J. Weigand, Combustion and Flame 139 (2004) 358-366.

[26] A. Osmont, L. Catoire, I. Gökalp, V. Yang, Combustion and Flame 151 (2007) 262-273.

[27] A. Burcat and B. Ruscic, Third Millennium Thermodynamic Database for Combustion and Air-Pollution Use with updates from Active Thermochemical Tables, updated on 9th February 2009.

[28] P. Dagaut, P. Glarborg, M.U. Alzueta, Progress in Energy and Combustion Science 34 (2008) 1-46.

[29] A.M. Dean, J.W. Bozzelli, in: W.C. Gardiner, Jr. (Ed.), Gas-Phase Combustion Chemistry, Springer-Verlag, New York, 2000, p. 125.

[30] Y. He, X. Liu, M.C. Lin, C.F. Melius, Int. J. Chem. Kinet. 25 (1993) 845-863.

[31] CHEMKIN-II: a Fortran chemical kinetics Package for the analysis of Gas-Phase Chemical and Plasma Kinetics, R.J.Kee, F.M. Rupley, E. Meeks, J. Miller, SAND96-8216, May 1996.

[32] SENKIN: a Fortran program for predicting homogeneous gas phase chemical kinetics with sensitivity analysis, A.E. Lutz, R.J. Kee, J.A. Miller, SAND87-8248, Feb. 1988.

[33] J.D. Mertens, A.J. Dean, R.K. Hanson, C.T. Bowman, Proc. Symp. Comb. 24 (1992) 701-710.

[34] J.D. Mertens, R.K. Hanson, Proc. Symp. Comb. 26 (1996) 551-558.

[35] J.D. Mertens, A.Y. Chang, R.K. Hanson, C.T. Bowman, Int. J. Chem. Kinet. 24 (1992) 279-295.

[36] J.D. Mertens, A.Y. Chang, R.K. Hanson, C.T. Bowman, Int. J. Chem. Kinet. 21 (1989) 1049-1067.

[37] M.S. Wooldridge, R.K. Hanson, C.T. Bowman, Int. J. Chem. Kinet. 28 (1996) 361-372.

## 7. Supplemental Information

Table of detailed chemical kinetics reaction model used in this work to simulate ignition delay times.

| | | | | |
|---|---|---|---|---|
| | | | ($k = A.\ T^b.\ \exp(-E/RT)$) | |
| REACTIONS CONSIDERED | | | A | b | E |
| 1. HCN+M = H+CN+M | | | 3.40E+35 | -5.1 | 133000.0 |
| | N2 | Enhanced by 0.000E+00 | | | |
| | O2 | Enhanced by 1.500E+00 | | | |
| | H2O | Enhanced by 1.000E+01 | | | |
| 2. HCN+N2=H+CN+N2 | | | 3.60E+26 | -2.6 | 124890.0 |
| 3. HCN+M=HNC+M | | | 1.60E+26 | -3.2 | 54600.0 |
| | AR | Enhanced by 7.000E-01 | | | |
| | H2O | Enhanced by 7.000E+00 | | | |
| | CO2 | Enhanced by 2.000E+00 | | | |
| 4. CN+H2=HCN+H | | | 1.10E+05 | 2.6 | 1908.0 |
| 5. HCN+O=NCO+H | | | 1.40E+04 | 2.6 | 4980.0 |
| 6. HCN+O=CN+OH | | | 4.20E+10 | 0.4 | 20665.0 |
| 7. HCN+O=NH+CO | | | 3.50E+03 | 2.6 | 4980.0 |
| 8. HCN+OH=CN+H2O | | | 3.90E+06 | 1.8 | 10300.0 |
| 9. HCN+OH=HOCN+H | | | 5.90E+04 | 2.4 | 12500.0 |
| 10. HCN+OH=HNCO+H | | | 2.00E-03 | 4.0 | 1000.0 |
| 11. HCN+OH=NH2+CO | | | 7.80E-04 | 4.0 | 4000.0 |
| 12. HCN+O2=CN+HO2 | | | 3.00E+13 | 0.0 | 75100.0 |

13. HCN+CN=NCCN+H 1.50E+07 1.7 1530.0

14. HNC+H=HCN+H 7.80E+13 0.0 3600.0

15. HNC+O=NH+CO 4.60E+12 0.0 2200.0

16. HNC+OH=HNCO+H 2.80E+13 0.0 3700.0

17. HNC+CN=NCCN+H 1.00E+13 0.0 0.0

18. CN+O=CO+N 1.90E+12 0.5 723.0

19. CN+OH=NCO+H 1.00E+15 -0.4 0.0

20. CN+O2=NCO+O 7.20E+12 0.0 -417.0

21. CN+O2=NCO+O ******** -2.0 0.0

22. CN+O2=NO+CO 2.80E+17 -2.0 0.0

23. CN+CO2=NCO+CO 3.70E+06 2.2 26900.0

24. CN+CH2O=HCN+HCO 4.20E+13 0.0 0.0

25. CN+NO=NCO+N 9.60E+13 0.0 42100.0

26. CN+NO2=NCO+NO 5.30E+15 -0.8 344.0

27. CN+NO2=CO+N2O 4.90E+14 -0.8 344.0

28. CN+NO2=N2+CO2 3.70E+14 -0.8 344.0

29. CN+HNO=HCN+NO 1.80E+13 0.0 0.0

30. CN+HONO=HCN+NO2 1.20E+13 0.0 0.0

31. CN+N2O=NCN+NO 3.80E+03 2.6 3700.0

32. CN+HNCO=HCN+NCO 1.00E+13 0.0 0.0

33. CN+NCO=NCN+CO 1.80E+13 0.0 0.0

34. HNCO+M=CO+NH+M 1.10E+16 0.0 86000.0

N2 Enhanced by 1.500E+00

35. HNCO+H=NH2+CO 3.60E+04 2.5 2345.0

36. HNCO+H=NCO+H2 9.00E+07 1.7 13900.0

37. HNCO+O=NCO+OH 2.20E+06 2.1 11430.0

38. HNCO+O=NH+CO2 9.60E+07 1.4 8520.0

39. HNCO+O=HNO+CO 1.50E+08 1.6 44012.0

40. HNCO+OH=NCO+H2O 3.60E+07 1.5 3600.0

41. HNCO+HO2=NCO+H2O2 3.00E+11 0.0 22000.0

42. HNCO+O2=HNO+CO2 1.00E+12 0.0 35000.0

43. HNCO+NH=NH2+NCO 3.00E+13 0.0 23700.0

44. HOCN+H=HNCO+H 3.10E+08 0.8 1917.0

45. HOCN+H=NH2+CO 1.20E+08 0.6 2076.0

46. HOCN+H=H2+NCO 2.40E+08 1.5 6617.0

47. HOCN+O=OH+NCO 1.70E+08 1.5 4133.0

48. HOCN+OH=H2O+NCO 1.20E+06 2.0 -248.0

49. HOCN+NH2=NCO+NH3 9.20E+05 1.9 3646.0

50. HCNO=HCN+O 4.20E+31 -6.1 61210.0

51. HCNO+H=HCN+OH 7.20E+10 0.8 8612.0

52. HCNO+O=HCO+NO 6.30E+13 0.0 0.0

53. HCNO+OH=CH2O+NO 1.00E+12 0.0 0.0

54. HCNO+O=NCO+OH 7.00E+12 0.0 0.0

55. HCNO+OH=NO+CO+H2 6.50E+12 0.0 0.0

56. HCNO+OH=NCO+H+OH 4.50E+12 0.0 0.0

57. HCNO+OH=NCO+H2O 3.50E+12 0.0 0.0

58. HCNO+OH=HCO+HNO 4.50E+12 0.0 0.0

59. NCO+M=N+CO+M 2.20E+14 0.0 54050.0

N2 Enhanced by 1.500E+00

60. NCO+H=CO+NH 7.20E+13 0.0 1000.0

61. NCO+O=NO+CO 2.00E+15 -0.5 0.0

62. NCO+OH=HON+CO 5.30E+12 -0.1 5126.0

63. NCO+OH=H+CO+NO 8.30E+12 -0.1 18042.0

64. NCO+HO2=HNCO+O2 2.00E+13 0.0 0.0

65. NCO+O2=NO+CO2 2.00E+12 0.0 20000.0

66. NCO+HCO=HNCO+CO 3.60E+13 0.0 0.0

67. CH2O+NCO=HNCO+HCO 6.00E+12 0.0 0.0

68. NCO+NO=N2O+CO 4.00E+19 -2.2 1743.0

69. NCO+NO=N2+CO2 1.50E+21 -2.7 1824.0

70. NCO+NO2=CO+NO+NO 2.50E+11 0.0 -707.0

71. NCO+NO2=CO2+N2O 3.00E+12 0.0 -707.0

72. NCO+HNO=HNCO+NO 1.80E+13 0.0 0.0

73. NCO+HONO=HNCO+NO2 3.60E+12 0.0 0.0

74. NCO+N=N2+CO 2.00E+13 0.0 0.0

75. NCO+NH3=HNCO+NH2 2.80E+04 2.5 980.0

76. NCO+NCO=CO+CO+N2 1.80E+13 0.0 0.0

77. H2CN=HCN+H 4.00E+28 -6.0 29897.0

78. H2CN+H=HCN+H2 2.40E+08 1.5 -894.0

79. H2CN+O=HCN+OH 1.70E+08 1.5 -894.0

80. H2CN+OH=HCN+H2O 1.50E+19 -2.2 2166.0

81. H2CN+OH=HCN+H2O 1.20E+06 2.0 -1192.0

82. H2CN+O2=CH2O+NO 3.00E+12 0.0 5961.0

83. H2CN+NH2=HCN+NH3 9.20E+05 1.9 -1152.0

84. HCNH=HCN+H 6.10E+28 -5.7 24271.0

85. HCNH+H=H2CN+H 2.00E+13 0.0 0.0

| | | | |
|---|---|---|---|
| 86. HCNH+H=HCN+H2 | 2.40E+08 | 1.5 | -894.0 |
| 87. HCNH+O=HNCO+H | 7.00E+13 | 0.0 | 0.0 |
| 88. HCNH+O=HCN+OH | 1.70E+08 | 1.5 | -894.0 |
| 89. HCNH+OH=HCN+H2O | 1.20E+06 | 2.0 | -1192.0 |
| 90. NH3+M=NH2+H+M | 2.20E+16 | 0.0 | 93470.0 |
| 91. NH3+H=NH2+H2 | 6.40E+05 | 2.4 | 10171.0 |
| 92. NH3+O=NH2+OH | 9.40E+06 | 1.9 | 6460.0 |
| 93. NH3+OH=NH2+H2O | 2.00E+06 | 2.0 | 566.0 |
| 94. NH3+HO2=NH2+H2O2 | 3.00E+11 | 0.0 | 22000.0 |
| 95. NH2+H=NH+H2 | 4.00E+13 | 0.0 | 3650.0 |
| 96. NH2+O=HNO+H | 6.60E+14 | -0.5 | 0.0 |
| 97. NH2+O=NH+OH | 6.80E+12 | 0.0 | 0.0 |
| 98. NH2+OH=NH+H2O | 4.00E+06 | 2.0 | 1000.0 |
| 99. NH2+HO2=H2NO+OH | 5.00E+13 | 0.0 | 0.0 |
| 100. NH2+HO2=NH3+O2 | 9.20E+05 | 1.9 | -1152.0 |
| 101. NH2+O2=H2NO+O | 2.50E+11 | 0.5 | 29586.0 |
| 102. NH2+O2=HNO+OH | 6.20E+07 | 1.2 | 35100.0 |
| 103. NH2+NH2=NH3+NH | 5.00E+13 | 0.0 | 10000.0 |
| 104. NH2+NH=NH3+N | 9.20E+05 | 1.9 | 2444.0 |
| 105. NH2+N=N2+H+H | 7.00E+13 | 0.0 | 0.0 |
| 106. NH2+NO=N2+H2O | 2.80E+20 | -2.7 | 1258.0 |
| 107. NH2+NO=NNH+OH | 2.30E+10 | 0.4 | -814.0 |
| 108. NH2+NO2=N2O+H2O | 1.60E+16 | -1.4 | 268.0 |
| 109. NH2+NO2=H2NO+NO | 6.50E+16 | -1.4 | 268.0 |
| 110. NH2+HNO=NH3+NO | 3.60E+06 | 1.6 | -1250.0 |

111. NH2+HONO=NH3+NO2 7.10E+01 3.0 -4940.0

112. NH+H=N+H2 3.00E+13 0.0 0.0

113. NH+O=NO+H 9.20E+13 0.0 0.0

114. NH+OH=HNO+H 2.00E+13 0.0 0.0

115. NH+OH=N+H2O 5.00E+11 0.5 2000.0

116. NH+O2=HNO+O 4.60E+05 2.0 6500.0

117. NH+O2=NO+OH 1.30E+06 1.5 100.0

118. NH+NH=N2+H+H 2.50E+13 0.0 0.0

119. NH+N=N2+H 3.00E+13 0.0 0.0

120. NH+NO=N2O+H 2.90E+14 -0.4 0.0

121. NH+NO=N2O+H ******** -0.2 0.0

122. NH+NO=N2+OH 2.20E+13 -0.2 0.0

123. NH+NO2=N2O+OH 1.00E+13 0.0 0.0

124. NH+HONO=NH2+NO2 1.00E+13 0.0 0.0

125. N+OH=NO+H 3.80E+13 0.0 0.0

126. N+O2=NO+O 6.40E+09 1.0 6280.0

127. N+NO=N2+O 3.30E+12 0.3 0.0

128. H2NO+M=HNO+H+M 2.80E+24 -2.8 64915.0

H2O Enhanced by 1.000E+01

129. H2NO+M=HNOH+M 1.10E+29 -4.0 44000.0

H2O Enhanced by 1.000E+01

130. H2NO+H=HNO+H2 3.00E+07 2.0 2000.0

131. H2NO+H=NH2+OH 5.00E+13 0.0 0.0

132. H2NO+O=HNO+OH 3.00E+07 2.0 2000.0

133. H2NO+OH=HNO+H2O 2.00E+07 2.0 1000.0

134. H2NO+HO2=HNO+H2O2 2.90E+04 2.7 1600.0

135. H2NO+O2=HNO+HO2 3.00E+12 0.0 25000.0

136. H2NO+NO=HNO+HNO 2.00E+04 2.0 13000.0

137. H2NO+NH2=HNO+NH3 3.00E+12 0.0 1000.0

138. H2NO+NO2=HONO+HNO 6.00E+11 0.0 2000.0

139. HNOH+M=HNO+H+M 2.00E+24 -2.8 58934.0

H2O Enhanced by 1.000E+01

140. HNOH+H=NH2+OH 4.00E+13 0.0 0.0

141. HNOH+H=HNO+H2 4.80E+08 1.5 378.0

142. HNOH+O=HNO+OH 7.00E+13 0.0 0.0

143. HNOH+O=HNO+OH 3.30E+08 1.5 -358.0

144. HNOH+OH=HNO+H2O 2.40E+06 2.0 -1192.0

145. HNOH+HO2=HNO+H2O2 2.90E+04 2.7 -1600.0

146. HNOH+O2=HNO+HO2 3.00E+12 0.0 25000.0

147. HNOH+NH2=NH3+HNO 1.80E+06 1.9 -1152.0

148. HNOH+NO2=HONO+HNO 6.00E+11 0.0 2000.0

149. HNO+H=NO+H2 4.40E+11 0.7 650.0

150. HNO+O=NO+OH 2.30E+13 0.0 0.0

151. HNO+OH=NO+H2O 3.60E+13 0.0 0.0

152. HNO+O2=HO2+NO 2.00E+13 0.0 16000.0

153. HNO+NO2=HONO+NO 6.00E+11 0.0 2000.0

154. HNO+HNO=N2O+H2O 9.00E+08 0.0 3100.0

155. HCO+HNO=NO+CH2O 6.00E+11 0.0 2000.0

156. HON+M=NO+H+M 5.10E+19 -1.7 16045.0

AR Enhanced by 7.000E-01

H2O Enhanced by 7.000E+00

CO2 Enhanced by 2.000E+00

157. HON+H=HNO+H 2.00E+13 0.0 0.0

158. HON+H=OH+NH 2.00E+13 0.0 0.0

159. HON+O=OH+NO 7.00E+13 0.0 0.0

160. HON+OH=HONO+H 4.00E+13 0.0 0.0

161. HON+O2=NO2+OH 1.00E+12 0.0 4968.0

162. H+NO(+M)=HNO(+M) 1.50E+15 -0.4 0.0

Low pressure limit: 0.23000E+15 0.20600E+00 -0.15500E+04

N2 Enhanced by 1.000E+00

H2O Enhanced by 1.000E+01

O2 Enhanced by 1.500E+00

H2 Enhanced by 2.000E+00

CO2 Enhanced by 3.000E+00

163. NO+O(+M)=NO2(+M) 1.30E+15 -0.8 0.0

Low pressure limit: 0.75000E+20 -0.14100E+01 0.00000E+00

N2 Enhanced by 1.700E+00

O2 Enhanced by 1.500E+00

H2O Enhanced by 1.000E+01

164. NO+OH(+M)=HONO(+M) 2.00E+12 -0.1 -721.0

Low pressure limit: 0.50000E+24 -0.25100E+01 -0.68000E+02

N2 Enhanced by 1.000E+00

O2 Enhanced by 1.000E+00

H2O Enhanced by 6.700E+00

AR Enhanced by 6.700E-01

165. NO+HO2=NO2+OH 2.10E+12 0.0 -480.0

166. HCO+NO=HNO+CO 7.00E+13 -0.4 0.0

167. HONO+H=HNO+OH 5.60E+10 0.9 5000.0

168. HONO+H=NO+H2O 8.10E+06 1.9 3850.0

169. HONO+O=NO2+OH 1.20E+13 0.0 6000.0

170. HONO+OH=NO2+H2O 4.00E+12 0.0 0.0

171. HONO+HONO=NO+NO2+H2O 3.50E-01 3.6 12100.0

172. NO2+H=NO+OH 1.30E+14 0.0 362.0

173. NO2+O=NO+O2 3.90E+12 0.0 -238.0

174. NO2+O(+M)=NO3(+M) 1.30E+13 0.0 0.0

Low pressure limit: 0.10000E+29 -0.40800E+01 0.24700E+04

N2 Enhanced by 1.500E+00

O2 Enhanced by 1.500E+00

H2O Enhanced by 1.000E+01

175. NO2+HO2=HONO+O2 6.30E+08 1.2 5000.0

176. NO2+H2=HONO+H 4.50E+12 0.0 27600.0

177. NO2+NO2=NO+NO+O2 1.60E+12 0.0 26123.0

178. NO2+NO2=NO3+NO 9.60E+09 0.7 20900.0

179. CO+NO2=CO2+NO 9.00E+13 0.0 33800.0

180. HCO+NO2=CO+NO+OH 1.20E+23 -3.3 2355.0

181. HCO+NO2=H+CO2+NO 8.40E+15 -0.8 1930.0

182. NO3+H=NO2+OH 6.00E+13 0.0 0.0

183. NO3+O=NO2+O2 1.00E+13 0.0 0.0

184. NO3+OH=NO2+HO2 1.40E+13 0.0 0.0

185. NO3+HO2=NO2+O2+OH 1.50E+12 0.0 0.0

186. NO3+NO2=NO+NO2+O2 5.00E+10 0.0 2940.0

187. NNH=N2+H 6.50E+07 0.0 0.0

188. NNH+H=N2+H2 1.00E+14 0.0 0.0

189. NNH+O=N2O+H 1.00E+14 0.0 0.0

190. NNH+O=N2+OH 8.00E+13 0.0 0.0

191. NNH+O=NH+NO 5.00E+13 0.0 0.0

192. NNH+OH=N2+H2O 5.00E+13 0.0 0.0

193. NNH+O2=N2+HO2 2.00E+14 0.0 0.0

194. NNH+O2=N2+H+O2 5.00E+13 0.0 0.0

195. NNH+NH=N2+NH2 5.00E+13 0.0 0.0

196. NNH+NH2=N2+NH3 5.00E+13 0.0 0.0

197. NNH+NO=N2+HNO 5.00E+13 0.0 0.0

198. N2O(+M)=N2+O(+M) 1.30E+12 0.0 62570.0

Low pressure limit: 0.40000E+15 0.00000E+00 0.56600E+05

N2 Enhanced by 1.700E+00

O2 Enhanced by 1.400E+00

CO2 Enhanced by 3.000E+00

H2O Enhanced by 1.200E+01

199. N2O+H=N2+OH 3.30E+10 0.0 4729.0

200. N2O+H=N2+OH 4.40E+14 0.0 19254.0

201. N2O+O=NO+NO 9.20E+13 0.0 27679.0

202. N2O+O=N2+O2 3.70E+12 0.0 15936.0

203. N2O+OH=N2+HO2 1.30E-02 4.7 36560.0

204. N2O+OH=HNO+NO 1.20E-04 4.3 25080.0

205. N2O+NO=NO2+N2 5.30E+05 2.2 46280.0

206. CO+N2O=N2+CO2 2.70E+11 0.0 20237.0

207. NCCN+M=CN+CN+M 1.10E+34 -4.3 130079.0

N2 Enhanced by 1.500E+00

O2 Enhanced by 1.500E+00

H2 Enhanced by 1.500E+00

H2O Enhanced by 1.000E+01

CO2 Enhanced by 3.000E+00

208. NCCN+O=CN+NCO 4.60E+12 0.0 8880.0

209. NCCN+OH=CN+HOCN 1.90E+11 0.0 2900.0

210. NO2+OH(+M)=HONO2(+M) 2.40E+13 0.0 0.0

Low pressure limit: 0.64000E+33 -0.54900E+01 0.23510E+04

N2 Enhanced by 1.000E+00

AR Enhanced by 7.000E-01

H2O Enhanced by 6.000E+00

211. H+H+M=H2+M 7.31E+17 -1.0 0.0

H2O Enhanced by 1.625E+01

CO Enhanced by 1.875E+00

CO2 Enhanced by 3.750E+00

212. O+O+M=O2+M 1.14E+17 -1.0 0.0

H2O Enhanced by 1.625E+01

CO Enhanced by 1.875E+00

CO2 Enhanced by 3.750E+00

213. O+H+M=OH+M 6.20E+16 -0.6 0.0

H2O Enhanced by 1.625E+01

CO Enhanced by 1.875E+00

CO2 Enhanced by 3.750E+00

214. H2+O2=OH+OH 1.70E+13 0.0 47780.0

215. O+H2=OH+H 3.87E+04 2.7 6260.0

216. H+O2=OH+O 4.40E+14 -0.1 16812.0

217. H+O2+M=HO2+M 8.00E+17 -0.8 0.0

H2O Enhanced by 1.000E+01

218. H+OH+M=H2O+M 8.62E+21 -2.0 0.0

H2O Enhanced by 1.625E+01

CO Enhanced by 1.875E+00

CO2 Enhanced by 3.750E+00

219. H2+OH=H2O+H 2.16E+08 1.5 3430.0

220. H2O+O=OH+OH 1.50E+10 1.1 17260.0

221. HO2+OH=H2O+O2 2.89E+13 0.0 -497.0

222. HO2+O=OH+O2 1.81E+13 0.0 -400.0

223. H+HO2=H2+O2 4.28E+13 0.0 1411.0

224. H+HO2=OH+OH 1.69E+14 0.0 874.0

225. H+HO2=H2O+O 3.01E+13 0.0 1721.0

226. HO2+HO2=H2O2+O2 4.08E+02 3.3 1979.0

227. OH+OH(+M)=H2O2(+M) 7.22E+13 -0.4 0.0

Low pressure limit: 0.22110E+20 -0.76000E+00 0.00000E+00

TROE centering: 0.50000E+00 0.10000E+09 0.10000E-05

228. H2O2+OH=HO2+H2O 5.80E+14 0.0 9557.0

229. H2O2+H=HO2+H2 1.70E+12 0.0 3750.0

230. H2O2+H=H2O+OH 1.00E+13 0.0 3590.0

231. H2O2+O=HO2+OH 2.80E+13 0.0 6400.0

232. CO+HO2=CO2+OH 1.50E+14 0.0 23650.0

233. CO+OH=CO2+H 4.40E+06 1.5 -740.0

234. CO+O+M=CO2+M 2.83E+13 0.0 -4540.0

H2O Enhanced by 1.625E+01

CO Enhanced by 1.875E+00

CO2 Enhanced by 3.750E+00

235. CO+O2=CO2+O 2.53E+12 0.0 47700.0

236. HCO+M=H+CO+M 1.85E+17 -1.0 17000.0

H2O Enhanced by 1.625E+01

CO Enhanced by 1.875E+00

CO2 Enhanced by 3.750E+00

237. HCO+OH=CO+H2O 1.00E+14 0.0 0.0

238. HCO+O=CO+OH 3.00E+13 0.0 0.0

239. HCO+O=CO2+H 3.00E+13 0.0 0.0

240. HCO+H=CO+H2 7.22E+13 0.0 0.0

241. HCO+O2=CO+HO2 4.72E+12 0.0 250.0

242. HCO+HO2=CO2+OH+H 3.00E+13 0.0 0.0

243. HCO+HCO=CH2O+CO 1.80E+13 0.0 0.0

244. HCO+HCO=H2+CO+CO 3.00E+12 0.0 0.0

245. CH2O+M=HCO+H+M 1.26E+16 0.0 77898.0

H2O Enhanced by 1.625E+01

CO Enhanced by 1.875E+00

CO2 Enhanced by 3.750E+00

246. CH2O+HO2=HCO+H2O2 4.00E+12 0.0 11665.0

247. CH2O+OH=HCO+H2O 1.72E+09 1.2 -447.0

248. CH2O+O=HCO+OH 1.81E+13 0.0 3088.0

249. CH2O+H=HCO+H2 1.26E+08 1.6 2170.0

250. CH2O+O2=HCO+HO2 2.04E+13 0.0 39000.0

251. HNCO+OH=NH2+CO2 6.30E+10 -0.1 11643.0

252. NCO+O=N+CO2 8.00E+12 0.0 2503.0

253. HNO+CH3=NO+CH4 8.20E+05 1.9 953.0

254. NO+C=CO+N 1.70E+13 0.0 0.0

255. NO+C=CN+O 1.10E+13 0.0 0.0

256. NH2+NO2=NH2NO2 3.50E+31 -6.8 3726.0

257. CH3O+NO=CH2O+HNO 8.40E+12 0.0 2050.0

258. CH3+HO2=CH3O+OH 2.28E+13 0.0 0.0

259. CH3+NO2=CH3O+NO 1.30E+13 0.0 0.0

260. N2O4(+M)=NO2+NO2(+M) 4.05E+18 -1.1 12840.0

Low pressure limit: 0.19600E+29 -0.38000E+01 0.12840E+05

261. NO2+HONO=NO+HONO2 6.03E+01 0.0 0.0

262. N2O4+H2O=HONO+HONO2 2.52E+14 0.0 11586.0

263. CO+OH(+M)=CO2+H(+M) 2.45E-03 3.7 -1242.8

Low pressure limit: 0.11700E+08 0.13500E+01 -0.71700E+03

264. HOCO(+M)=CO2+H(+M) 1.74E+12 0.3 32935.0

Low pressure limit: 0.22900E+27 -0.30200E+01 0.35062E+05

265. HOCO(+M)=CO+OH(+M) 5.89E+12 0.5 33986.6

Low pressure limit: 0.21900E+24 -0.18900E+01 0.35277E+05

266. CHCO+M=CO+CH+M 6.00E+15 0.0 58819.3

267. CH+O=CO+H 1.00E+14 0.0 0.0

268. CH+OH=HCO+H 3.00E+13 0.0 0.0

269. CH+O2=CO+OH 2.00E+13 0.0 0.0

270. CH2S+O=CO+H+H 1.50E+13 0.0 0.0

271. CH2S+O=CO+H2 1.50E+13 0.0 0.0

272. CH2S+OH=CH2O+H 3.00E+13 0.0 0.0

273. CH2S+O2=CO+OH+H 3.10E+13 0.0 0.0

274. CH2T+O=CO+H+H 5.00E+13 0.0 0.0

275. CH2T+OH=CH+H2O 1.13E+07 2.0 3011.5

276. CH2T+OH=CH2O+H 2.50E+13 0.0 0.0

277. CH2T+O2=CO2+H+H 1.60E+12 0.0 1003.8

278. CH2T+O2=CH2O+O 5.00E+13 0.0 9010.5

279. CH2T+O2=CO2+H2 6.90E+11 0.0 501.9

280. CH2T+O2=CO+OH+H 8.60E+10 0.0 -501.9

281. CH2T+O2=HCO+OH 4.30E+10 0.0 -501.9

282. CH3+O=CH2O+H 8.43E+13 0.0 0.0

283. CH3+OH=CH2O+H2 8.00E+12 0.0 0.0

284. CH3+OH=CH2T+H2O 1.13E+06 2.1 2437.8

285. CH3+O2=CH2O+OH 5.20E+13 0.0 34894.8

286. CH3+O2=CH3O2 1.70E+60 -15.1 18785.8

287. CH3+HCO=CH4+CO 3.20E+11 0.5 0.0

288. CH3OH=CH3+OH 2.80E+32 -5.0 97992.3

289. CH4+HO2=CH3+H2O2 4.48E+13 0.0 24641.5

290. CH3+HO2=CH4+O2 1.00E+12 0.0 0.0

291. CH4+O=CH3+OH 1.90E+09 1.4 8675.9

292. CH4+OH=CH3+H2O 1.50E+06 2.1 2437.8

293. CH3CHO=HCO+CH3 2.00E+15 0.0 79110.9

294. HCO+CH3OH=CH2O+CH2OH 9.60E+03 2.9 13097.5

295. CH2O+CH3=HCO+CH4 8.91E-13 7.4 -956.0

296. CH2O+M=CO+H2+M 8.20E+15 0.0 69550.7

H2 Enhanced by 2.900E+00

O2 Enhanced by 1.200E+00

N2 Enhanced by 1.200E+00

H2O Enhanced by 1.850E+01

CO Enhanced by 2.100E+00

CO2 Enhanced by 4.300E+00

297. CH3O+M=CH2O+H+M 1.96E+37 -6.7 33269.6

H2 Enhanced by 2.900E+00

O2 Enhanced by 1.200E+00

N2 Enhanced by 1.200E+00

H2O Enhanced by 1.850E+01

CO Enhanced by 2.100E+00

CO2 Enhanced by 4.300E+00

298. CH2OH+M=CH2O+H+M 1.54E+13 0.0 33054.5

H2 Enhanced by 2.900E+00

O2 Enhanced by 1.200E+00

N2 Enhanced by 1.200E+00

H2O Enhanced by 1.850E+01

CO Enhanced by 2.100E+00

CO2 Enhanced by 4.300E+00

299. CH2OH+H=CH3+OH 9.64E+13 0.0 0.0

300. CH2OH+H=CH2O+H2 3.00E+13 0.0 0.0

301. CH2OH+O=CH2O+OH 5.00E+12 0.0 0.0

302. CH2OH+OH=CH2O+H2O 5.00E+12 0.0 0.0

303. CH2OH+HO2=CH2O+H2O2 1.20E+13 0.0 0.0

304. CH2OH+CH3=CH2O+CH4 2.40E+12 0.0 0.0

305. CH2OH+HCO=CH2O+CH2O 1.80E+14 0.0 0.0

306. CH2OH+HCO=CH3OH+CO 1.20E+14 0.0 0.0

307. CH2OH+O2=CH2O+HO2 1.80E+13 0.0 788.7

308. CH2OH+H2O2=CH3OH+HO2 3.01E+09 0.0 2581.3

309. CH3OH+O2=CH2OH+HO2 2.00E+13 0.0 44909.2

310. CH3+OH=CH3O+H 5.74E+12 -0.2 13934.0

311. CH3+O2=CH3O+O 4.30E+13 0.0 30807.8

312. CH3O+H=CH2O+H2 2.00E+13 0.0 0.0

313. CH3O+O=CH2O+OH 5.00E+12 0.0 0.0

314. CH3O+OH=CH2O+H2O 5.00E+12 0.0 0.0

315. CH3O+O2=CH2O+HO2 4.28E-13 7.6 -3537.3

316. CH3O+HO2=CH2O+H2O2 1.20E+13 0.0 0.0

317. CH3O+CH3=CH4+CH2O 2.41E+13 0.0 0.0

318. CH3O+CH2O=HCO+CH3OH 1.15E+11 0.0 1290.6

319. CH3O2H=CH3O+OH 6.46E+14 0.0 42997.1

320. CH3OH+OH=CH2OH+H2O 1.77E+04 2.6 -884.3

321. CH3OH+OH=CH3O+H2O 1.77E+04 2.6 -884.3

322. CH3OH+H=CH2OH+H2 3.20E+13 0.0 6094.6

323. CH3OH+H=CH3O+H2 8.00E+12 0.0 6094.6

324. CH3OH+H=CH3+H2O 5.25E+12 0.0 5329.8

325. CH3OH+O=CH2OH+OH 3.88E+05 2.5 3083.2

326. CH3OH+CH3O=CH2OH+CH3OH 1.51E+12 0.0 7002.9

327. CH3OH+C2H3=CH2OH+C2H4 3.20E+01 3.2 7170.2

328. CH3O2+H=CH3O+OH 9.60E+13 0.0 0.0

329. CH3O2+O=CH3O+O2 3.60E+13 0.0 0.0

330. CH3O2+OH=CH3OH+O2 6.00E+13 0.0 0.0

331. CH3O2+HO2=CH3O2H+O2 4.60E+10 0.0 -2581.3

332. CH3O2+HCO=CH3O+H+CO2 3.00E+13 0.0 0.0

333. CH3O2+CH3=CH3O+CH3O 2.00E+13 0.0 0.0

334. CH3O2+H2O2=CH3O2H+HO2 2.40E+12 0.0 9942.6

335. CH3O2+CH2O=CH3O2H+HCO 2.00E+12 0.0 11663.5

336. CH3O2+CH3O2=CH3O+CH3O+O2 7.80E+10 0.0 0.0

337. CH3O2+CH3O2=CH3OH+CH2O+O2 1.30E+11 0.0 0.0

338. CH3O2+CH4=CH3O2H+CH3 1.80E+11 0.0 18475.1

339. CH3O2+H2=CH3O2H+H 3.00E+13 0.0 26027.7

340. CH3O2+CH3OH=CH3O2H+CH2OH 1.80E+11 0.0 13719.0

341. CH3O2H+OH=CH3O2+H2O 7.00E+12 0.0 1434.0

342. CH3O2H+O=CH3O2+OH 2.80E+13 0.0 6405.3

343. C2H+O=CO+CH 1.00E+13 0.0 0.0

344. C2H+OH=CHCO+H 2.00E+13 0.0 0.0

345. C2H+O2=CHCO+O 6.02E+11 0.0 0.0

346. C2H+O2=CH+CO2 4.50E+15 0.0 25095.6

347. C2H+O2=HCO+CO 2.41E+12 0.0 0.0

348. C2H2+OH=C2H+H2O 2.71E+13 0.0 10492.3

349. CHCO+H=CH2S+CO 1.50E+14 0.0 0.0

350. CHCO+O=CO+CO+H 1.00E+14 0.0 0.0

351. C2H2+O=CH2T+CO 7.81E+03 2.8 501.9

352. C2H2+O=CHCO+H 1.39E+04 2.8 501.9

353. C2H2+OH=HCCOH+H 5.06E+05 2.3 13503.8

354. C2H2+OH=CH2CO+H 2.19E-04 4.5 -1003.8

355. C2H2+OH=CH3+CO 4.85E-04 4.0 -2007.6

356. HCCOH+H=CH2CO+H 1.00E+13 0.0 0.0

357. CH2CO+H=CHCO+H2 3.00E+13 0.0 8604.2

358. CH2CO+O=HCO+HCO 1.00E+13 0.0 5975.1

359. CH2CO+OH=CHCO+H2O 1.00E+13 0.0 2629.0

360. CH2CO=CH2T+CO 3.00E+14 0.0 70984.7

361. C2H3+OH=C2H2+H2O 4.00E+12 0.0 0.0

362. C2H3+O=CH2CO+H 3.00E+13 0.0 0.0

363. C2H3+O2=CH2O+HCO 3.98E+12 0.0 -239.0

364. CH3CO+H=CH2CO+H2 2.00E+13 0.0 0.0

365. CH3CO+O=CH3+CO2 2.00E+13 0.0 0.0

366. CH3CO+CH3O2=CH3+CO2+CH3O 2.40E+13 0.0 0.0

367. C2H4+HO2=C2H3+H2O2 1.12E+13 0.0 30425.4

368. C2H4+O2=C2H3+HO2 3.98E+13 0.0 61496.2

369. C2H3+CH3OH=C2H4+CH3O 1.40E+01 3.1 6931.2

370. C2H4+O=CH3+HCO 1.60E+08 1.4 525.8

371. C2H4+O=CH3CO+H 1.60E+08 1.4 525.8

372. C2H4+O=C2H3+OH 7.11E+08 1.6 7480.9

373. C2H4+OH=C2H3+H2O 9.70E+06 1.9 2361.4

374. CH3CHO+H=CH3CO+H2 4.00E+13 0.0 4206.5

375. CH3CHO+O=CH3CO+OH 5.00E+12 0.0 1792.5

376. CH3CHO+OH=CH3CO+H2O 1.00E+13 0.0 0.0

377. CH3CHO+CH3=CH3CO+CH4 8.50E+10 0.0 6000.0

378. CH3+CH2OH=C2H5+OH 1.37E+14 -0.4 6596.6

379. C2H5+O=CH2O+CH3 4.24E+13 0.0 0.0

380. C2H5+O=CH3CHO+H 5.32E+13 0.0 0.0

381. C2H5+O=C2H4+OH 3.06E+13 0.0 0.0

382. C2H5+O2=C2H4+HO2 2.00E+12 0.0 4995.2

383. C2H5+CH3OH=C2H6+CH2OH 3.20E+01 3.2 9153.9

384. C2H6+CH3O2=C2H5+CH3O2H 3.00E+11 0.0 14937.9

385. C2H6+HO2=C2H5+H2O2 1.70E+13 0.0 20458.9

386. C2H6+O2=C2H5+HO2 3.98E+13 0.0 50908.2

387. C2H6+O=C2H5+OH 1.40E+00 4.3 2772.5

388. C2H6+OH=C2H5+H2O 2.20E+07 1.9 1123.3

389. C2H5+CH3OH=C2H6+CH3O 1.40E+01 3.1 8938.8

390. N2H2+O=NH2+NO 1.00E+13 0.0 0.0

391. N2H2+O=NNH+OH 3.30E+08 1.5 497.0

392. N2H2+OH=NNH+H2O 2.40E+06 2.0 -600.0

393. N2H2+NO=NH2+N2O 4.00E+12 0.0 11922.0

394. NO2+O=NO3 1.32E+13 0.0 0.0

395. NH2+O2=NH+HO2 1.00E+14 0.0 49997.0

396. NH2+NO=N2O+H2 5.00E+13 0.0 24481.0

397. NH+O=N+OH 1.70E+08 1.5 3368.0

398. NH2+O=NO+H2 5.00E+12 0.0 0.0

399. CH4(+M)=CH3+H(+M) 2.40E+16 0.0 104913.6

Low pressure limit: 0.45000E+18 0.00000E+00 0.90806E+05

TROE centering: 0.10000E+01 0.10000E+03 0.13500E+04 0.78300E+04

400. CH3NH+OH=CH2NH+H2O 3.60E+06 2.0 -1192.0

401. CH3NH+O=CH2NH+OH 5.00E+08 1.5 -894.0

402. CH3NH+O2=CH2NH+HO2 1.00E+07 2.0 6300.0

403. CH3NH+O=CH3O+NH 6.00E+13 0.0 0.0

404. CH3NH+OH=CH4+HNO 6.00E+12 0.0 0.0

405. CH3NH+O2=CH3O+HNO 6.00E+12 0.0 4000.0

406. CH2NH+O=CH2O+NH 1.70E+06 2.1 0.0

407. CH2NH+OH=CH2O+NH2 1.80E+05 2.0 14800.0

408. CH2NH+O=H2CN+OH 1.70E+08 1.5 4630.0

409. H2CN+HO2=CH2NH+O2 1.40E+04 2.7 -1609.0

410. CH2NH+OH=H2CN+H2O 1.20E+06 2.0 -89.0

411. H2CN+O2=HCN+HO2 2.70E+04 2.0 17300.0

412. H2CN+NO=HCN+HNO 1.00E+07 2.0 4400.0

413. CH3+CH3(+M)=C2H6(+M) 3.61E+13 0.0 0.0

Low pressure limit: 0.12600E+42 -0.70000E+01 0.27619E+04

TROE centering: 0.62000E+00 0.73000E+02 0.11800E+04

414. CH2NH+M=HCN+H2+M 1.00E+14 0.0 10000.0

415. 2H+H2=H2+H2 9.20E+16 -0.6 0.0

416. NH2+NH=N2H2+H 1.50E+15 -0.5 0.0

417. N2H2+M=NNH+H+M 5.00E+16 0.0 50000.0

418. N2H2+H=NNH+H2 4.80E+08 1.5 1580.0

419. N2H2+NH=NNH+NH2 2.40E+06 2.0 -1192.0

420. N2H2+NH2=NH3+NNH 1.80E+06 1.9 -1152.0

421. 2NH2=N2H2+H2 5.00E+11 0.0 0.0

422. CH4+H=CH3+H2 1.30E+04 3.0 8037.0

423. CH4+CH2T=CH3+CH3 4.30E+12 0.0 10036.0

424. CH3+M=CH2T+H+M 1.00E+16 0.0 90607.0

425. CH3+H=CH2S+H2 6.00E+13 0.0 15101.0

426. CH3+H=CH2T+H2 9.00E+13 0.0 15101.0

427. CH3+CH3=C2H5+H 3.01E+13 0.0 13512.0

428. CH2T+H=CH+H2 6.00E+12 0.0 -1788.0

429. CH2T+CH2T=C2H2+H2 1.20E+14 0.0 795.0

430. CH2T+CH3=C2H4+H 4.20E+13 0.0 0.0

431. CH2T+CH=C2H2+H 4.00E+13 0.0 0.0

432. CH2T+C2H6=CH3+C2H5 6.50E+12 0.0 7910.0

433. CH2S+N2=CH2T+N2 6.00E+12 0.0 0.0

434. CH2S+CH4=CH2T+CH4 7.20E+12 0.0 0.0

435. CH2S+C2H2=CH2T+C2H2 4.80E+13 0.0 0.0

436. CH2S+C2H4=CH2T+C2H4 1.38E+13 0.0 0.0

437. CH2S+C2H6=CH2T+C2H6 2.16E+13 0.0 0.0

438. CH2S+CH4=2CH3 4.00E+13 0.0 0.0

439. CH2S+C2H6=CH3+C2H5 1.20E+14 0.0 0.0

440. CH+CH4=C2H4+H 6.00E+13 0.0 0.0

441. CH+CH3=C2H3+H 3.00E+13 0.0 0.0

442. C2H6=C2H5+H 2.08E+38 -7.1 106507.0

443. C2H6+H=C2H5+H2 1.41E+09 1.5 7402.0

444. C2H6+CH3=C2H5+CH4 3.97E+05 2.5 17684.0

445. C2H5+H=C2H4+H2 1.25E+14 0.0 8000.0

446. C2H5+CH3=C2H4+CH4 4.36E-04 5.0 8300.0

447. C2H5+C2H5=C2H4+C2H6 1.40E+12 0.0 0.0

448. C2H4+M=C2H2+H2+M 3.00E+17 0.0 79349.0

449. C2H4+M=C2H3+H+M 2.91E+17 0.0 96558.0

450. C2H4+H=C2H3+H2 5.40E+14 0.0 14902.0

451. C2H4+H=C2H5 1.05E+14 -0.5 655.0

452. C2H4+C2H4=C2H5+C2H3 5.00E+14 0.0 64700.0

453. C2H4+CH3=C2H3+CH4 4.14E+12 0.0 11127.0

454. C2H3+H=C2H2+H2 1.20E+13 0.0 0.0

455. C2H3+CH3=C2H2+CH4 4.36E-04 5.0 8300.0

456. C2H3+C2H6=C2H4+C2H5 1.50E+13 0.0 10000.0

457. C2H3+C2H3=C2H2+C2H4 1.08E+13 0.0 0.0

458. C2H3+CH2T=C2H2+CH3 3.00E+13 0.0 0.0

459. C2H3+CH=CH2T+C2H2 5.00E+13 0.0 0.0

460. C2H2+C2H2=C2H3+C2H 9.64E+12 0.0 84448.0

461. C2H2+H=C2H+H2 6.00E+13 0.0 27818.0

462. C2H2+CH3=C2H+CH4 1.81E+11 0.0 17287.0

463. C2H2+M=C2H+H+M 4.20E+16 0.0 107000.0

464. CH+N2=HCN+N 4.40E+12 0.0 21976.0

465. CN+N=C+N2 2.40E+13 0.0 -556.0

466. CH2T+N2=HCN+NH 1.00E+13 0.0 74000.0

467. H2CN+N=N2+CH2T 2.00E+13 0.0 0.0

468. H2CN+M=HCN+H+M 3.00E+14 0.0 22000.0

469. CH2T+N=HCN+H 5.00E+13 0.0 0.0

470. CH+N=CN+H 1.70E+14 -0.1 0.0

471. CH3+N=H2CN+H 6.10E+14 -0.3 288.0

472. C2H3+N=HCN+CH2T 2.00E+13 0.0 0.0

473. CN+HCN=C2N2+H 1.50E+07 1.7 1530.0

474. NH3+HONO2=H2O+NH2NO2 8.00E-01 3.5 43100.0

475. HONO2+OH=H2O+NO3 9.00E+10 0.0 0.0

476. HONO2+H=NO3+H2 5.60E+08 1.5 16400.0

477. HONO2+O=OH+NO3 1.80E+07 0.0 0.0

478. HNCO+N=NH+NCO 2.32E+19 0.0 52500.0

479. HNCO+NO3=CO2+NO+HNO 1.00E+12 0.0 9996.0

480. HNCO+NO2=CO2+HNNO 2.51E+12 0.0 26000.0

481. HNCO+M=H+NCO+M 1.00E+17 0.0 112000.0

482. N2O+NCO=CO+N2+NO 9.00E+13 0.0 27800.0

483. NO+M=N+O+M 1.40E+15 0.0 148429.0

484. HNCO+CH3=NCO+CH4 1.00E+12 0.0 9935.0

485. NO2+N=N2O+O 3.49E+12 0.0 -437.0

486. CH+N2=NCN+H 2.22E+07 1.5 23367.0

487. H+NCN=HCN+N 1.89E+14 0.0 8425.0

488. NCN+N=CN+N2 2.00E+13 0.0 0.0

489. C2N2+O=NCO+CN 4.57E+12 0.0 8880.0

490. HNO+NO+NO=HNNO+NO2 1.70E+11 0.0 2100.0

491. HNNO+NO=NNH+NO2 3.20E+12 0.0 270.0

492. HNNO+NO=N2+HONO 2.60E+11 0.0 810.0

493. HNNO+M=H+N2O+M 2.20E+15 0.0 21600.0

494. HNNO+M=N2+OH+M 1.00E+15 0.0 25600.0

495. HNNO+OH=H2O+N2O 2.00E+13 0.0 0.0

496. HNNO+H=H2+N2O 2.00E+13 0.0 0.0

497. HONO2+H=NO2+H2O 6.00E+13 0.0 9800.0

498. HONO2+H=HONO+OH 2.00E+13 0.0 8000.0

499. HONO2+OH(+M)=H2O+NO3(+M) 2.47E+08 0.0 -2860.0

Low pressure limit: 0.68900E+15 0.00000E+00 -0.14400E+04

N2O Enhanced by 5.000E+00

H2O Enhanced by 9.000E+00

HONO2 Enhanced by 5.000E+00

NO3 Enhanced by 5.000E+00

NH3 Enhanced by 5.000E+00

500. NO3+H2O2=HONO2+HO2 1.00E+12 0.0 8500.0

501. HONO+NO3=HONO2+NO2 1.00E+12 0.0 6000.0

502. NO3+NO3=NO2+NO2+O2 5.12E+11 0.0 4870.0

503. HNNO+NO=N2O+HNO 1.00E+12 0.0 0.0

504. HNNO+NO2=N2O+HONO 1.00E+12 0.0 0.0

505. HNNO+NO2=NNH+NO3 1.00E+13 0.0 0.0

506. HNCO+HONO2=CO2+H2O+N2O 1.00E+05 0.0 0.0

NOTE: A units in $cm^3\ mole^{-1} cm^3\ sec^{-1}$, T in K and, E in cal $mole^{-1}$.